J Solid State Electrochem (2017) 21:2467–2488
DOI 10.1007/s10008-016-3472-4

REVIEW

The renaissance in redox flow batteries

M. K. Ravikumar[1] · Suman Rathod[1] · Nandini Jaiswal[1] · Satish Patil[1] · Ashok Shukla[1]

Received: 16 September 2016 / Revised: 6 November 2016 / Accepted: 10 November 2016 / Published online: 23 November 2016

Abstract Although redox flow batteries were invented as early as 1954, no system development took place until NASA demonstrated an Fe/Cr redox flow battery system in 1970s. In hibernation for several years, redox flow battery systems have begun to catch the attention of policy makers globally. The resurrection of redox flow batteries rests heavily on their techno-economic feasibility as large-scale energy storage systems for emerging grid network that are being developed by climate change mitigation industries, namely, wind and solar. This article reviews various redox flow battery technologies with a cost and market prognosis.

Introduction

The invention of steam engine by James Watt was an important contribution to ignite the industrial revolution of eighteenth century. Subsequently, the steam engines evolved into steam turbines that were coupled with a dynamo to generate electric power. The invention of power generation using steam turbines led to rapid growth of several power stations across the globe. Fossil fuels were used to generate the steam to produce electric power in these power stations. At present, about 68 % of world's electric power generation capacity is met from fossil fuels [1]. Continuous exploitation of fossil fuels over a period of about 100 years has caused in their depletion with increased pollution of our environment. World population at the beginning of the industrial revolution was 700 million which is presently pegged at about 7 billion and is expected to reach 9 billion by 2050 [2]. The demand for electrical energy is continually growing both due to an increase in population and rapid industrialization. International Energy Agency (IEA) has projected that the world's energy demand will increase from about ~12 billion tonne-oil equivalent in 2009 to 18 billion tonne-oil equivalent by 2035 based both on "ACT-now-scenario" and "BLUE-map-scenario" [1]. ACT-now-scenario projections are based on technologies, which already exist or in advanced stages of development and that can bring down CO_2 emissions back to current levels by 2050. BLUE map scenario projections are based on the development of technologies that could bring down CO_2 emissions from 50 to 80 % by 2050 and will confine global warming to about 2 °C [1]; this is also referred to as 2DS target.

The world requires another revolution in power generation from sources other than fossil fuels to bring down their use and to achieve 2DS target. Grids connected with renewable energy sources (RES) are expected to contribute in achieving the 2DS target by providing flexibility in electricity systems and reducing wastage of thermal energy. However, direct integration of renewable energy sources with the central grids has several issues. Firstly, electricity presently being generated from power stations has a balance in demand and supply. Secondly, these power stations are located in distant places and generated power is distributed to the consumer through a grid network. Renewable energy sources like wind and solar energy are highly intermittent and depend on weather conditions. Wind energy output decreases on days without wind and also in certain times the power output fluctuates with gust and turbulence. Similarly, solar energy is generated only from dawn to dusk. Moreover, solar power output fluctuates due to the passing clouds. These power fluctuations will put stress on the central grid if it is directly integrated to renewable energy

✉ Ashok Shukla
akshukla2006@gmail.com

[1] Solid State and Structural Chemistry Unit, Indian Institute of Science, Bangalore 560012, India

grids. Hence, it is mandatory to store electrical energy from the renewable energy sources in electrical energy storage systems (EES) and use it adequately for regulated power supply.

The best option for integrating renewable energy sources with main grid is to develop "local grids" involving RES and EES. The local grid is divided into different categories, namely, pico grids, nano grids, micro grids, and milli grids, based on the nature of their functions and control system or electric load. There are different reported and recommended definitions for different category of local grids [3–5]. They generally represent branches of main grid with an RES, EES, and loads connected to them and also have the capability to work independent of main grid. They differ from each other in terms of magnitude of the power load that they can manage and associated power control systems. A pico grid may be defined as a single home or gadget connected with a power generation system such as Solar PVs and a UPS [3, 4]. The typical load range of a pico grid may be 0–10 kW. Such a pico grid can be developed for taking responsibility of peak shaving and time shifting applications. A nano grid is defined as single power domain system with single voltage, single frequency, reliability, quality, capacity, and administration [3]. The typical power load range of nano grid may be 10 to 100 kW. They can be responsible for peak shaving, time shifting, and emergency backup power load management and energy efficiency applications [4]. Nano grids are suitable for commercial and large residential buildings. According to the DoE recommendations, a micro grid may be defined as a group of interconnected loads and distributed energy resources within clearly defined electrical boundaries that act as single controllable entity with respect to grid. A micro grid can connect and disconnect from the main grid to enable it to operate in both grid connection and island mode [3]. The typical range of power load for a micro grid may be in the range of 100 kW–10 MW.

Current scenario for energy storage is promising, but high capital cost of storage technologies precludes their widespread deployment. Large-scale energy storage systems established using different technologies were sized for over 145 GW in 2014 [7]. It is estimated that by the year 2050, about 310 GW of additional grid-connected electricity storage capacity would be needed only in the USA, Europe, China, and India [6]. The most important feature of the 2DS scenario is clean electricity with renewable energy technologies which would increase their contribution to global electricity generation from 20 to 65 % by 2050 [6]. A micro grid is developed to manage large distributed energy resources and control systems. They can be used in load leveling, voltage regulation and control, energy trading, resiliency, aggregation, and telecommunication applications in addition to what other smaller grids can do. A milli grid, also termed as a mini grid, is similar to micro grid but with a higher power range of 10–100 MW. Mini grids are more suitable for spinning reserve, nonspinning reserve, load leveling, transmission and distribution stability, load following, and black start applications. The envisaged local grid structure is represented in Fig. 1.

The choice of energy storage system is found in applications that they offer at varying locations of the main grid. Desired characteristics for energy storage systems in few specific applications and power demand are reported elsewhere [6]. Grid categorization of these applications with power demand is presented in Table 1 and Fig. 2. The desired characteristics and power demand suitability of an energy storage system for a specific application can be broadly evaluated from the electrical characteristics of the energy storage system. Among these characteristics, power demand and total energy requirement for a specific application are most important. Power demand and required discharge time vary with the nature of the application. Figure 2 shows power demand against discharge time to illustrate situations that are most suited for specific applications along with the proposed categorization of local grids. It is wise to choose a particular category of local grid and an appropriate EES for integrating a RES with main grid for a specific application. The development of different categories of local grid with appropriate selection of RES and EES is the key to success of integrating renewable energy source with main grid and thereby reducing the greenhouse gas emission.

International Energy Agency has recommended a road map for various energy storage technologies for harnessing energy from renewable energy sources. There are four major challenges in widespread utilization of energy storage technologies, namely, (a) establishing cost-competitive energy storage technologies including production and grid integration, (b) validated reliability, (c) safety to environment, and (d) industrial and public acceptance of these technologies [8]. It is projected that such an energy storage system would help bridging the prevailing gap in the integration of local grid with the main grid. There are many energy technologies that could meet the above characteristics and that are being developed for applications listed in Table 2. EES is generally classified into mechanical, electrical, chemical, electrochemical, and thermal energy storage systems, which are widely accepted for electrical energy storage in the local grids [9].

These technologies have reached varying levels of maturity. A comparison of techno-economic features of these power generation technologies with their current status of commercialization along with other potential electrochemical systems is presented in Table 2 [10–13] along with their suitability for local grid development. The energy storage systems like pumped hydroelectric storage and compressed air energy storage systems have required characteristics for developing milli grids. But these systems are site centric and hence are limited due to the requirement of specific geographic locations. Accordingly, these systems have widespread installations. Among other energy storage systems listed in Table 2, electrochemical energy storage systems have many benefits,

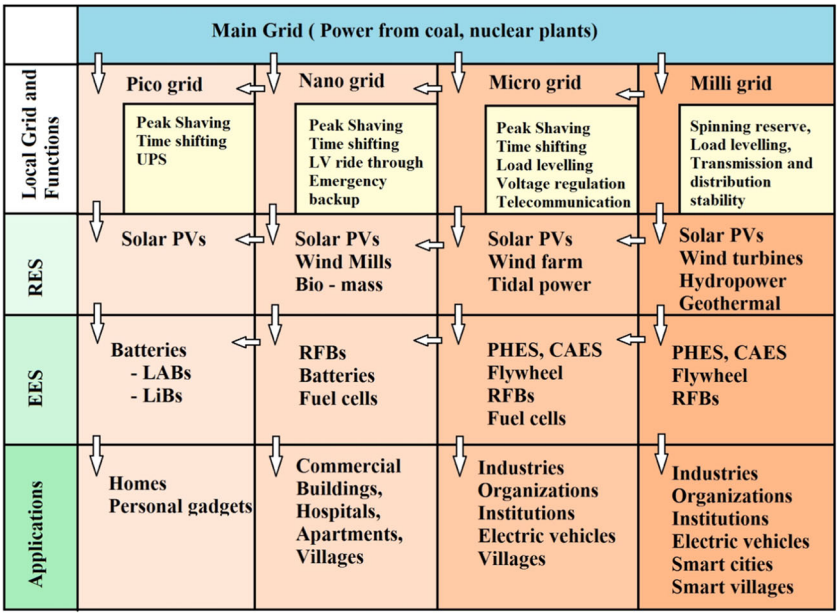

Fig. 1 Envisaged structure of the local grid

namely, flexibility in design and size. These are not site centric and can be built at any place. Also, as indicated, electrochemical systems such as batteries, supercapacitors, and redox flow batteries for storing electrical energy can meet the required quality of power and energy with desired response time that are needed to develop micro, nano, and pico grids. Among the various types of electrochemical energy storage systems, redox flow batteries have several benefits over conventional batteries and supercapacitors.

An attractive feature of the redox flow battery (RFB) systems is that the power and energy density are independent of each other in contrast to batteries and supercapacitors. The power (kW) of the system is determined by the size of the electrodes and the number of cells in a stack, while the energy storage capacity (kWh) is determined by the concentration and volume of the electrolyte. This special feature helps in building RFB systems with large-scale energy storage suitable for developing micro and nano grids. In the wake of growing demand for the development of pico, nano, and micro grids, we have reviewed various types of RFB systems after describing their working principle, brief history, and classification in this review paper.

Table 1 Important characteristic of energy storage systems for specific applications with grid categorization

Grid category	Size of EES/power demand (MW)	Discharge duration	Cycles/day	Response time	Application
Pico	0.001–0.01	3–5 h	1–2	<1 h	Off-grid
Pico	0.001–0.01	5 min to 3 h	1–29	<15 min	Peak shaving and time shifting
Pico	0.001–0.01	>30 min	1–5	<few seconds	UPS/emergency backup
Nano	0.01–0.1	3–5 h	1–2	<5 h	Off-grid
Nano	0.01–0.1	5 min to 3 h	1–29	<15 min	Demand shifting and peak reduction
Micro	1–40	1 s to 1 min	10–100	0.001–1 s	Voltage support
Micro	0.1–10	5 min to 3 h	1–30	<15 min	Peak shaving, time shifting, demand shifting
Micro/milli	1 to 500	2–5 h	0.75 to 1.25	<1 h	Transmission and distribution infrastructure investment deferral
Micro/milli	1 to 400	1 min to 12 h	0.5–2	<15 min	Variable supply resource integration
Micro/milli	10–500	2–4 h	0.14–1.25	<1 h	Transmission and distribution congestion relief
Micro/milli/mini	1–2000	1 to 15 min	20–40	<1 h	Frequency regulation, spinning reserve, nonspinning reserve
Micro/milli/mini	1–2000	1–24 h	1–2	<1 h	Arbitrage
Micro/milli/mini	1–2000	Days–months	1–5/year	<day	Seasonal storage
Micro/milli/mini	0.1–2000	1–4 h	<1/year	<1 h	Black start

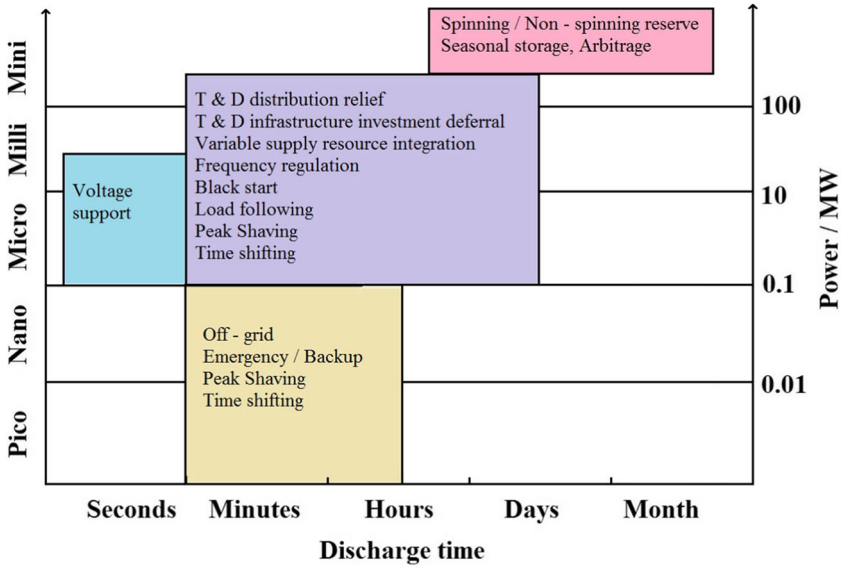

Fig. 2 Power demand vs. discharge duration for specific applications and envisaged local grid categorization

Redox flow batteries

A conventional rechargeable battery like lead-acid battery or Li-ion battery stores the chemical energy in the form of active materials in electrodes. During charge and discharge of such batteries, the electrode materials undergo oxidation and reduction reactions. Hence, the quantum of electrical energy stored in such batteries is confined to the quantity of active materials stored in the electrodes. By contrast to this, in redox flow batteries, the chemical energy is stored in electrolyte in dissolved form of active materials. Hence, a redox flow battery is a form of rechargeable battery in which electrolyte containing one or more dissolved species flows through an electrochemical cell that converts chemical energy directly into electrical energy. Additional electrolyte is stored externally, generally in tanks, and is usually pumped through the cell or stack of cells of the reactor although gravity-feed systems are also known. Flow batteries can be rapidly recharged by replacing the liquid electrolyte akin to filling fuel tanks for internal combustion engines while simultaneously recovering the spent materials for re-energizing. The schematic description of a redox flow cell is shown in Fig. 3.

As shown in Fig. 3, a RFB consists of an anode and a cathode with fluid-flow fields separated by a suitable ion exchange membrane. The flow cell is connected to two electrolyte reservoirs and two pumps are used to circulate the electrolyte through the flow cell. The electrolyte circulated through anode is called anolyte (or negolyte), while the electrolyte circulated through cathode is called catholyte (or posolyte). The anolyte and the catholyte are different redox solutions which flow or are pumped past inert electrodes. The spent solutions are retained in storage tanks, and the whole process is reversed during charge. The general cell reaction is thus:

$$A_{red}(aq) + B_{ox}(aq) \overset{\text{Discharge}}{\rightarrow} A_{ox}(aq) + B_{red}(aq)$$
$$A_{ox}(aq) + B_{red}(aq) \overset{\text{Charge}}{\rightarrow} A_{red}(aq) + B_{ox}(aq)$$

The used electrolyte depleted in the concentration of active materials can also be pumped into the reactant tank itself. Although the used electrolyte can be pumped into the reactant tank itself, there are few benefits in collecting the used electrolyte in separate tanks, namely, (i) when reactant electrolyte concentration remains constant, RFB can deliver a constant power output. If we collect the product electrolyte into the reactant electrolyte, the concentration of the active material will decrease with time and hence the cell voltage will decrease due to concentration polarization. (ii) The reactant electrolyte level in the tank directly indicates SoC of the RFB when separate electrolyte tanks are used for reactant and products. The flow of the electrolyte can be controlled by opening the respective on/off valves during charge/discharge as shown in Fig. 3. Indeed, Enervault's *Engineered Cascade*™-based RFB systems are unique in that the cell stacks are connected hydrolytically in series for the delivery of constant power under steady-state operating conditions and efficiency as long as the charged electrolyte and discharged electrolytes are stored separately and pumped into the *Engineered Cascade*™ RFB system [14].

Liquid electrolytes in reservoirs store the energy chemically which are circulated through the cell during charging, and the stored chemical energy is converted back to electrical energy when discharged. Electrolyte solutions are prepared by dissolving electrochemically active materials in a suitable supporting electrolyte, such as sulfuric acid, to minimize the

Table 2 Comparison of different energy storage devices with the redox flow battery

Energy storage technology	Power rating (MW)	Discharge duration (h)	Response time	Efficiency (without power electronics)	Energy density Wh/kg	Power density W/kg	Capital cost ($/kWh)	Cycle cost ($/kWh) output	Life (years)	Cycle life at 80 % DoD	Maturity	Safety issues	Local grid category
Pumped hydroelectric storage	10–5000	1–24	Very good	70–85 %	0.5–1.5		80–200	0.001–0.02	50–60	20,000–50,000	C	Exclusion area	Milli grid, micro grid
SMES	10 MW	0.25	Good	90–95 %	0.5–5	500–2000	10,000	0.4–1.70	15–20	1000–10,000	C	Magnetic field	Milli grid, micro grid
Compressed air energy storage	10 MW to GW	0.1–15	Very good	60–79			50–110	0.03–0.06 (with gas)	20–40	9000–30,000	LC	Pressure vessels	Micro grid, milli grid
Flywheel energy storage	1–100 kW	0.1–1	Slow	>90 %	5–100	1000	300–5000	0.05–0.4	15–20	>20,000	C	Containment	Micro grid, nano grid
Supercapacitors	5–100 kW	0.02–1	Good	>95 %	0.05–10	500–2000	82,000	0.03–0.4	5–8	10,000–100,000	C		Nano grid
Thermal energy storage	Up to 100 MW	1–45	Slow	60 %			$500/kW	0.035–0.16	20	4000–10,000	C	High temperature	Milli grid, micro grid
Lead-acid batteries	kW to 10 MW	0.1–4	Fast	70–76 %	30–50	1000	350–1500	0.40–1	5–10	200–1500	C	Fire accidents due to hydrogen	Pico grid, nano grid
Sodium–sulfur batteries	0.1–100 MW	1–10	Fast	85–90 %	150–250	150–230	300–950	0.09–0.5	5–10	210–4500	DC	High temperature and potential fires	Nano grid, micro grid
Lithium-ion batteries	KWs to 100 MW	0.1–1	Fast	>90 %	150–350	50–2000	850–5000	0.3–1	5–15	5000–7000	DC	Potential fires and explosions	Pico grid,

C commercial, *LC* limited commercial, *DC* demonstrated at commercial

solution resistance. The flow cell is charged from an external dc power source to produce electrochemically active redox couples. Renewable energy sources such as solar or wind energy can also be used as external power to charge the redox flow batteries. Since the two electrolytes have two redox couples with different electrochemical potentials, a cell voltage is developed when the charged electrolyte is circulated through the flow cell which acts as power source for performing useful work. When an electric load is connected across the anode and cathode terminals, electrons flow from the anode to cathode and the chemical energy stored in the electrolyte is converted into electrical energy. It is the free energy change of the overall cell reaction which is converted into electrical energy ($-\Delta G^{o} = nFE^{o}$). Accordingly, the energy stored in the solutions is determined by the concentration of the electrochemically active materials and the volume of the reservoir. However, the power rating of the flow cell is determined by the number of cells in the cell stack and their electrode area. Thus, the power and energy density of such RFB systems are independent of each other.

RFB systems have a number of attractive traits, especially the flexibility of capacity and power output as capacity can be increased simply by enlarging the size or number of storage tanks while power output can be raised by increasing the area of the electrode and number of cells. Other benefits of RFBs in large-scale energy storage are listed below.

1. The electrode reactions are fast and provide good reversibility.
2. They are operated at room temperature.
3. RFBs are safe to operate.
4. Electrodes do not take part in charge and discharge reactions and hence they offer a high life cycle.
5. They can be operated both in deep discharge mode and partial state-of-charge mode without any difficulties.
6. They have fast response time.
7. They offer high coulombic efficiency of nearly 99 %.
8. They also offer high overall energy efficiency.
9. Their development is not restricted to any specific geographical land requirements.
10. Since the energy is stored in electrolytes which are stored in separate tanks, the rate of self-discharge is very low.

Unlike a fuel cell where the electrolyte remains at all times within the reactor for example in the form of an ion exchange membrane, in a redox flow cell, at least some of the electrolyte and generally the majority of the electrolyte in weight and volume terms flows through the reactor. Flow batteries are also distinguished from the fuel cell as the chemical reactions involved in a redox flow cell are often reversible that are generally of the rechargeable battery type and so can be recharged without replacing the electroactive chemicals.

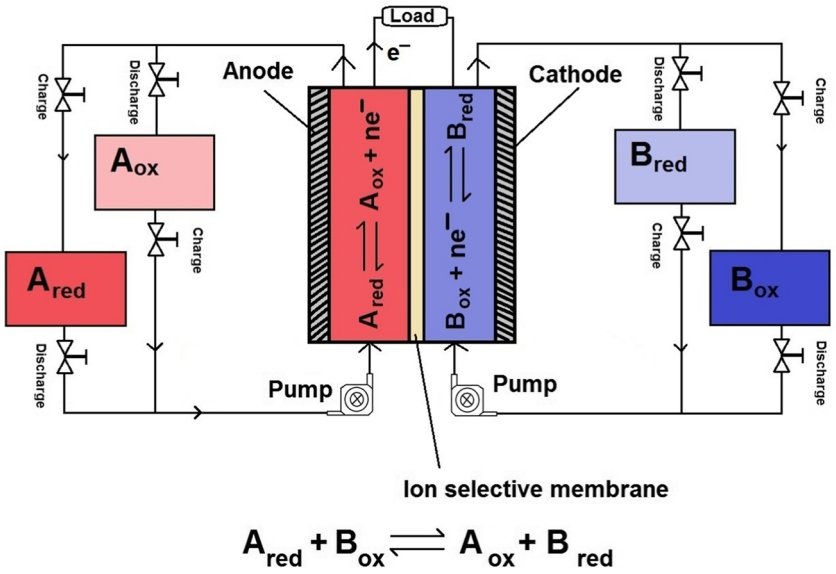

Fig. 3 Schematic description of a redox flow cell

Historical background

In the past, several battery systems have been used for personal and domestic needs, but in recent years, lithium batteries have shown great promise in mobile applications, particularly in laptops, mobile phones, and electric vehicles. However, these batteries are unsuitable for large-scale energy storage due to their cycle life and high cost. The desire for an eco-friendly large-scale electrochemical energy system for harnessing the renewable energy has grown since 2005. This has renewed the interest in the R&D of redox flow batteries [15–42]. The historical background and timeline of the invention of various types of RFBs are reviewed elsewhere [29, 37]. In brief, the concept of storing electrical energy in electrolyte in a redox flow cell was first invented by Walter Kangro in 1954. He filed a patent for storing energy in electrolytes using Fe^{3+}/Fe^{2+}, Cr^{6+}/Cr^{3+}, Ti^{4+}/Ti^{4+}, and Cl^{-}/Cl_2 redox couples. However, no system was developed. In 1970s, NASA developed Fe/Cr redox flow battery system and reported many other possible redox flow batteries. It is only in 1986 that all vanadium redox flow battery reported by Skyllas-Kazacos et al. brought RFB systems as a forefront technology for large-scale energy storage. Redox flow batteries have been known for nearly 40 years now with about hundred different types of RFB systems being developed and evaluated by various groups around the world currently. The taxonomy of different RFB system is described in the following section.

Taxonomy of redox flow batteries

RFBs can be broadly classified into two types based on chemical nature of electrolytes as (i) aqueous electrolyte RFBs and (ii) nonaqueous electrolyte RFBs. Each of the two types of RFBs can be further divided into three categories depending on the physical nature of the electrochemically active material, namely, (a) redox flow batteries with both the active materials of anode and cathode in dissolved state, for example all vanadium redox flow battery, iron–chromium redox flow battery, etc., (b) redox flow batteries with one of the two active materials in solid state, for example zinc–bromine redox flow battery, and (c) redox flow batteries with both the anode and cathode active materials in solid state, for example soluble lead redox flow battery. The taxonomy of RFBs is presented in Table 3.

Among the various RFB systems, only a few systems have reached the level of pilot-scale development. The widespread commercialization of the advanced stage RFBs is hindered due to problems like high cost, requirement of periodical maintenance, and technical issues. We have discussed the status of some RFB systems with current developments in the following sections. All other RFB systems are mainly developed with an academic interest and their details are reviewed elsewhere [37]. Vanadium redox flow battery system is the only RFB system that has reached pilot-scale development. Other systems that are in advanced level of development are Fe/Cr redox flow batteries and polysulfide-bromine redox flow batteries, zinc–bromine redox flow batteries (ZBRFBs), and soluble lead-acid redox flow batteries (SLRFB). Zinc–bromine system is not strictly a redox flow battery since the Zn electrode half-cell reactions involve deposition/dissolution of Zn. These RFB systems are also called “hybrid” redox flow batteries since one of the two electrodes is similar to battery electrodes. These are reviewed in this report due to their similarity in design and operation with redox-flow battery. SLRFB system is based on the deposition of Pb and PbO_2 at the anode and cathode from the lead salts. Such a battery was first reported by Fritz Beck [43]. Fritz Beck reported the development of lead perchlorate cells by depositing Pb and

Table 3 Taxonomy of the redox flow battery

Aprotic and ionic liquid/nonaqueous electrolytes

Single phase (all liquid)	Two phase (hybrid)	Two phase (liquid/gas)	Single phase (all liquid)	Two phase (suspensions, nanofluids, etc.)
$V^{3+}/V^{2+}//VO^{2+}/VO_2^+$	$Zn^{2+}/Zn//Ni^{2+}/Ni$	$H^+/H_2//Br_2/Br^-$	$[Ru(bpy)_3]^{2+}/[Ru(bpy)_3]^+//[Ru(bpy)_3]^{2+}/[Ru(bpy)_3]^{3+}$	$LiCoO_2$//LTO
$V^{3+}/V^{2+}//Fe^{3+}/Fe^{2+}$	$Zn^{2+}/Zn//Br_2/Br^-$	$H^+/H_2//Cl_2/Cl^-$	$[Ni(bpy)_3]^{2+}/[Ni(bpy)_3]//[Fe(bpy)_3]^{2+}/[Fe(bpy)_3]^{3+}$	$2Li^+/Li$//15D3GAQ/15GA3Q^{2-}
$V^{3+}/V^{2+}//ClBr_2^-/Br^-$	$Zn^{2+}/Zn//Cl_2/Cl^-$	$H^+/H_2//Fe^{3+}/Fe^{2+}$	$[Ru(acac)_3]/[Ru(acac)_3]^-//[Ru(acac)_3]/[Ru(acac)_3]^+$	$LiFePO_4$//LTO
$V^{3+}/V^{2+}//Ce^{4+}/Ce^{3+}$	$Zn^{2+}/Zn//ClBr_2^-/Br^-$	$H^+/H_2//VO^{2+}/VO_2^+$	$[V(acac)_3]/[V(acac)_3]^-//[V(acac)_3]/[V(acac)_3]^+$	$Li^+/Li//Fe^{3+}/Fe^{2+}$
$Cr^{3+}/Cr^{2+}//Fe^{3+}/Fe^{2+}$	$Zn^{2+}/Zn//VO^{2+}/VO_2^+$		$[Cr(acac)_3]/[Cr(acac)_3]^-//[Cr(acac)_3]/[Cr(acac)_3]^+$	Na/EMICI-Fe
$Cr^{3+}/Cr^{2+}//Br_2/Br^-$	$Zn^{2+}/Zn//Ce^{4+}/Ce^{3+}$		$[Mn(acac)_3]/[Mn(acac)_3]^-//[Mn(acac)_3]/[Mn(acac)_3]^+$	Cu/Cu (DEA-EHN)
$Cr^{3+}/Cr^{2+}//CrO_4^{2-}/Cr^{3+}$	$V^{3+}/V^{2+}//O_2/O^{2-}$		U(acac)	$CuCl_4^{2-}/CuCl_3^{2-}$//Cu/$CuCl_3^{2-}$
$S/S^{2-}//Br_2/Br^-$	$Fe^{2+}/Fe//Fe^{3+}/Fe^{2+}$		$[Co(acacen)]/[Co(acacen)]^-//[Co(acacen)]/[Co(acacen)]^+$	
$[SiV_3{}^{IV}W_9{}^{VI}O_{40}]^{10-}/$	$Cd^{2+}/Cd//Br_2/Br^-$		$[TEMPO]/[TEMPO]^+//[NMPI]/[NMPI]^-$	
$[SiV_3{}^{IV}W_3{}^{V}W_6{}^{VI}O_{40}]^{13-}$	$Pb^{2+}/Pb//PbO_2/Pb^{2+}$		DBBB/TMQFe^{3+}-TEA/Fe^{2+}-TEA//Br_2/Br^-	
$//[SiV_3{}^{IV}W_9{}^{VI}O_{40}]^{10-}/$	CuCl/Cu//Cu^{2+}/CuCl			
$[SiV_3{}^{V}W_3{}^{VI}O_{40}]^{7-}$	$Cu^{2+}/Cu//PbO_2/Pb^{2+}$			
$TiO^{2+}/Ti^{3+}//Fe^{3+}/Fe^{2+}$	$Zn^{2+}/Zn//PANI$			
$TiO^{2+}/Ti^{3+}//ClBr_2^-/Br^-$	$Cd^{2+}/Cd//Chloranil$			
$Np^{4+}/Np^{3+}//NpO_2{}^{2+}/NpO_2^+$	$Pb^{2+}Pb//Tiron$			
$I_2/I^-//IO_3^-/I_2$	V^{3+}/V^{2+}//Glyoxal/Glyoxlic acid			
Fe^{3+}/Fe^{2+}-EDTA//Br_2/Br^-	V^{3+}/V^{2+}//L-cysteine/L-cysteine acid			
Quinone//Br_2/Br^-				
Cr^{3+}/Cr^{2+}-EDTA//Cr^{5+}/Cr^{3+}-EDTA				

Chloranil tetrachloro-*p*-benzoquinone, *Tiron* (1,2-dihydroxybenzene-3,5-disulfonic acid), *EDTA* ethylene diaminetetraacetic acid, *PANI* polyaniline, *bpy* 2,2′-bipyridine, *Acac* acetylacetonate, *Acacen* (4E,4′E)-4,4′-(1,2-ethandiyldinitrilo) di (2-pentanonyl), *TEMPO* 2,2,6,6-tetramethyl-1-piperidinyloxy, *NMPI* *N*-methylphthalimide, *DBBB* 2,5-di-tert-butyl-1,4-bis(2-methoxyethoxy) benzene, *TMQ* 2,3,6-trimethylquinoxaline, *TEA* triethanolamine, *15D3GAQ* 1,5-bis{2-[2-(2-methoxyethoxy)ethoxy]ethoxy} anthracene-9,10-dione, *LTO* lithium titanate, *EMICI* 1-ethyl-3-methylimidazolium chloride, *DEA* diethanolamine, *EHN* 2-ethylhexanoate

PbO_2 from solution containing lead perchlorate salt dissolved in perchloric acid solution. A more recent SLRFB system developed by Pletcher et al. in 2004 is based on lead methanesulfonate salts and is described in a later section.

General performance and characteristics of RFBs

In general, the voltage of the cell decreases from the theoretical cell voltages or open-circuit voltage when the RFBs are discharged. This difference in voltage is called polarization or overpotential. The charge and discharge curves are generally divided into three regions as shown schematically in Fig. 4. Region I called activation overpotential is due to activation energy barrier associated with the charge transfer reaction at the electrode–electrolyte interface. Region II is called ohmic overpotential and is due to the internal resistance of the RFB. Region III is called concentration overpotential and is due to concentration gradient of the electroactive species at the electrode–electrolyte interface. The general current–overpotential equation defining the performance behavior of the RFBs is given by,

$$i = i_o\left[\left(1-\frac{i}{i_{l,c}}\right)e^{-\alpha f\eta}-\left(1-\frac{i}{i_{l,a}}\right)e^{(1-\alpha)f\eta}\right]$$

where i is current, i_o is the exchange current density, $i_{l,c}$ is cathode limiting current, $i_{l,a}$ is the anode liming current, η is the overpotential, f is equal to RT/F, and α is the transfer coefficient. It is desirable to have at least a 50-mA/cm^2 current density within a loss of 10 % of overpotential of RFBs. This would result in about 80 % energy efficiency of the RFB. Flow batteries are characterized by its voltage (V), energy storage capacity (Ah), power (W) coulombic efficiency (η_C), voltaic efficiency (η_V), and energy efficiency (η_E) at specified operating condition of the flow battery. Other important characteristics of the RFBs are cycle life and self-discharge.

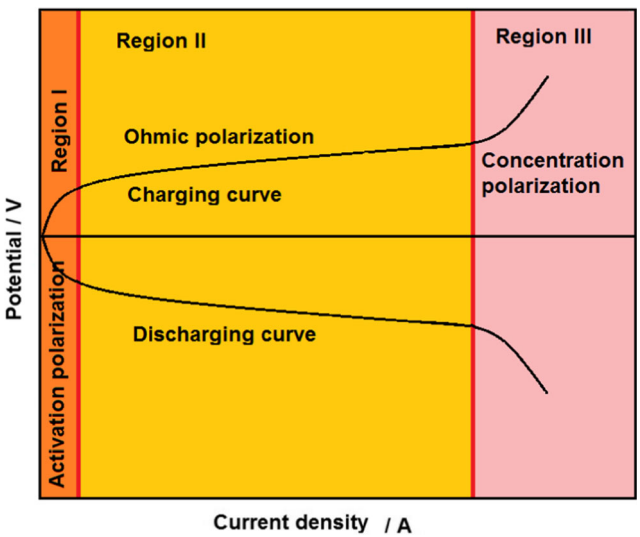

Fig. 4 A schematic representation of polarization curve of a battery

The voltage (V) of the RFB depends on the half-cell potentials of the anolyte, catholyte, and number of cells connected in series. The power output of the RFB is the product of current and voltage at a specified time. It is given by $W = I \times V$. The average power output is given by

$$\overline{W} = \frac{\int_0^t IV\,dt}{t}$$

where W is the mean power output, I is the instantaneous current, V is the instantaneous voltage, and t is the time. The energy storage capacity of the RFB depends on the concentration and volume of the electrolyte under specific flow rate, rate of charge, and discharge conditions. The active materials dissolved in the electrolyte are not completely utilized to deliver all the capacity. Hence, the energy storage capacity is often represented by utilization rate of the electrolyte and it is defined as the ratio between the practical capacity delivered to the theoretical capacity of the RFB.

$$\eta = \frac{Q_{\text{practical}}}{Q_{\text{theoretical}}} \times 100\% = \frac{W_{\text{practical}}}{W_{\text{theoretical}}} \times 100\%$$

where η is the utilization rate of energy capacity, Q is the capacity, and W is the power output.

The coulombic efficiency is the ratio between output charge (C) to the input charge and is obtained by,

$$\eta_C = \frac{C_{\text{output}}}{C_{\text{input}}} \times 100\%$$

where η_C is coulombic efficiency, C_{input} is charge input in coulombs (As), and C_{output} is the charge output in coulombs. Coulombic efficiency will decrease if there is any crossover of the electrolyte across the ion exchange membrane. Hence, it is an important characteristic of the RFB. The voltaic efficiency is the ratio between average discharge voltage and average charging voltage and it is given by,

$$\eta_v = \frac{V_{\text{discharge}}}{V_{\text{charge}}} \times 100\%$$

where η_V is the voltaic efficiency and V_{charge} and $V_{\text{discharge}}$ are charging and discharging voltage of the RFB. The energy efficiency is the ratio between the output energy and input energy and is given by,

$$\eta_E = \frac{W_{\text{discharge}}}{W_{\text{charge}}} \times 100\%$$

where η_E is the voltaic efficiency and W_{charge} and $W_{\text{discharge}}$ are charging and discharging energy in watts (W) of the RFB.

Status and recent developments in RFB systems

All vanadium redox flow batteries

Among the various RFBs, only all vanadium redox flow batteries have reached the level of pilot-scale demonstration. There are many desired features involved in the development of all vanadium redox flow battery (VRFB) systems as listed below.

1. In general, the voltage of an electrochemical cell depends on the nature of the electrolyte. In aqueous acidic electrolytes, such as sulfuric acid and hydrochloric acid, water is stable up to a potential of 1.23 V. The thermodynamic stability of water depends on the nature of electrode material. In the case of platinized platinum anode, hydrogen evolution is assumed to take place at 0 V. This electrode is used as primary reference electrode.

$$\text{At anode} \qquad 2H^+ + 2e^- \rightleftarrows H_2 \quad E^\circ = 0\,\text{V}$$

$$\text{At cathode} \qquad H_2O \rightleftarrows \frac{1}{2}O_2 + 2\text{H}^+ + 2e^- \quad E^\circ = 1.23\,\text{V}$$

When graphitic carbon is used as an electrode, these two reactions take place at high overpotential. The hydrogen evolution occurs at more negative potentials than −0.4 V vs. Standard Hydrogen Electrode (SHE) and oxygen evolution occurs above 1.6 V vs. (SHE) [37].

2. Vanadium is stable in four different oxidation states forming two redox couples: an anode potential of −0.26 V vs. SHE and cathode potential of 1.00 V vs. SHE adding to a single cell potential of 1.26 V. Both the anolyte and catholyte can be charged within overpotential regime of hydrogen evolution and oxygen evolution reactions. Accordingly, the water is not electrolyzed and remains stable during the operation of the VRFB.
3. Vanadium salts have solubilities close to 3 M. The desired optimum concentration of vanadium salts in sulfuric acid is 2 M. The electrode reactions are one-electron transfer reactions. Since 1 mol of electronic charge corresponds to 26.8 Ah, with 2 mol of acid in the electrolyte being utilized with close to 100 % coulombic efficiency and single cell potential close to 1 V, the electrolytes have nearly 50 Wh/l of volumetric energy density and or 50 Wh/kg of gravimetric energy density.

Vanadium in +2 and +3 oxidation states makes a redox couple at anode while in +4 as vanadyl ion (VO^{2+}) and +5 as dioxovandadium cation (VO_2^+) oxidation states makes another redox couple at cathode. In vanadium RFBs, the energy storage is realized through the electrochemical reactions involving one electron transfer across the interface. The electrochemical reactions for vanadium redox flow battery (VRFB) with the thermodynamic reference potentials can be written as:

At anode:

$$VO^{2+} + H_2O \rightleftarrows VO_2^+ + 2H^+ + e^- \rightarrow E_a^{\,o} = -0.26\ \text{V vs.SHE}$$

At cathode:

$$V^{3+} + e^- \rightleftarrows V^{2+} \qquad E_c^{\,o} = 1.00\ \text{vs.SHE}$$

The overall cell reaction:

$$VO^{2+} + V^{3+} + H_2O \rightleftarrows VO_2^+ + V^{2+} + 2H^+ \quad E_{cell}^{\,o} = E_c^{\,o} - E_a^{\,o} = 1.26\ \text{V}$$

The operating principle of all VRFB is similar to Fig. 3 where redox couple A_{red}/A_{ox} represents redox couple VO^{2+}/VO_2^+ and B_{red}/B_{ox} represents V^{2+}/V^{3+}.

Electrodes

The most commonly employed electrode material is graphite. This is because graphite has (a) good electrical conductivity, (b) is chemically stable in acids, and (c) can be obtained in different forms such as carbon cloth, carbon paper, carbon foams, and carbon felts. However, other metallic electrodes such as Au, Sn, Ti, Pt-Ti, and IrO-Ti have also been used. The electrochemical reversibility is not sufficient on Au electrodes. Sn and Ti electrodes are passivated in acidic medium and, with passive film-covered surface, they exhibit high resistance. Pt-Ti and IrO-Ti electrodes show good electrochemical activity with no passive layer formation. However, such electrodes are very expensive. Carbon electrodes in the form of carbon felts prepared from nonwoven carbon fibers are found to be the most suitable electrode material. But the carbon felt electrodes show poor electrochemical activity towards electrode reactions. The electrochemical activity of carbon felt electrode can be improved by activating them by various methods. Various methods that are reported for activating the carbon electrodes are as follows:

1. Heat treatment of the carbon electrodes at 400 °C for 30 h
2. Chemical treatment of the carbon electrodes in NaOCl, $KMnO_4$, and $(NH_4)_2S_2O_8$
3. Combined heat and acid treatment: The carbon felt electrodes were treated with sulfuric acid or nitric acid for 5 h and then heat treated in air at 450 °C for 2 h
4. Electrochemical oxidation of the carbon felt electrodes
5. Metal doping of the carbon electrodes: Metal doping is carried out by impregnating method. Carbon electrodes impregnated with Pt4+, Pd2+, Au4+, Ir3+, Mn2+, and In3+ have been reported that show better performance than the unimpregnated carbon. Among the various

metals reported, Ir^{3+} shows the best electrochemical activity towards the charge and discharge reactions.

Flow field plates

Since a single cell produces only 1.62 V, several cells are connected in series to achieve desired voltages. This requires the electrolyte to be circulated through all the cells. In order to minimize volume of the system and effective circulation of the electrolyte, bipolar plates are employed to realize high-voltage systems. The bipolar plates need to have the following characteristics:

1. Good electrical conductivity to reduce the internal resistance of the battery
2. High mechanical strength to withstand compression force and support the electrode
3. Good chemical resistance to acids and oxidizing atmosphere
4. Easy to fabricate

Metal plates, graphite plates, and composite graphite plates have been studied. Among these, plates with nonprecious metals show poor chemical stability and get passivated. These can be corrosion resistive but they lack durability. Metals like platinum, gold, and titanium show all desired properties but are highly expensive. Graphitic bipolar plates although meet the desired properties, they have porous structure resulting in shorting between the anolyte and catholyte during prolonged operation. Although nonporous high-density graphite can be made, the process is time consuming and costly. Carbon composite plates are being used at present. These are made from graphite, and the porous structures are filled with polymer to make them impervious. The flow fields are usually optimized using computational fluid dynamics.

Proposed mechanism for the increased activity with carbon electrodes

At cathode–catholyte interface, the charging reaction involves oxidation of vanadyl ions, VO^{2+}, to dioxovanadium cation, VO_2^+. This reaction requires an oxygen atom that needs to come from water molecules. However, graphitic carbon being a hydrophobic material does not attract water molecules to the close proximity of the electrode. Adsorption of water molecules on carbon surface takes place only at high overpotentials. When carbon electrodes are subjected to any one of the aforesaid methods, they develop functional groups such as C–OH, COOH, etc. The presence of such functional groups provides active sites for oxidation of vanadyl ions. Varying mechanisms have been proposed by different investigators for electrode reactions of VRFBs. These reaction mechanisms can be summarized in four steps. The first step involves diffusion of V ions from the bulk of the electrolyte to electrode surface and its adsorption. In the second step, an ion exchange taking place between the V ions and the protons of the functional groups at active sites. In the third step, electron transfer and oxygen transfer take place at cathode while only electron transfer takes place at anode. Subsequently, in the final fourth step, an ion exchange process takes place between the adsorbed V ions and protons of the electrolyte. The reaction products diffuse into the bulk of the electrolyte [25, 37, 44]. It is noteworthy that the exact mechanism is still a subject of discussion, and further investigations by in situ spectroscopic methods are required.

Electrolyte separator

Vanadium redox flow batteries are developed using graphite felt electrodes and a proton exchange membrane as separator. Proton exchange membranes, such as Nafion 117, Nafion 112, etc., can be used between the anolyte vanadous sulfate (VSO_4) and catholyte. Vanadyl sulfate ($VOSO_4$) dissolved in sulfuric acid. Typically, 2 mol of $VOSO_4$ is used in 2 M solution of sulfuric acid.

A proton exchange membrane is used as an electrolyte separator. The desired characteristics of the electrolyte separator are as follows:

1. High ion selectivity
2. High ionic conductivity
3. High chemical resistance to oxidizing agents like, VO_2^+
4. High mechanical strength
5. Low cost

Nafion is the most commonly employed ion exchange membrane in the development of RFBs. The abbreviation for Nafion is sodium (Na) fast ion conductor. Na^+ is exchanged with H^+ to make a proton exchange membrane. Nafion is the perflourosulfonic acid polymer. It has a $–(CF_2\text{-}CF\text{-})_x–(CF_2\text{-}CF_2)_y–$ chain as backbone to the polymer with a side chain of $–(O\text{-}CF_2\text{-}CF(CF_3)\text{-}O\text{-}CF_2CF_2\text{-}SO_3H$ as shown below:

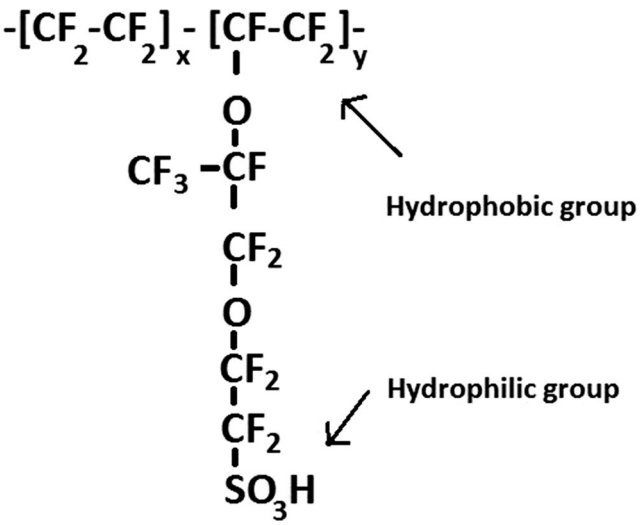

Among Nafion membranes, Nafion 117 and Nafion 115 are the most commonly employed membranes. Although Nafion membranes are found to have good ionic conductivity, chemical resistance, and desired mechanical properties, they are prone to crossover of vanadium ions resulting in loss of energy efficiency. In order to improve the ion selectivity and water balance, Nafion is modified by various methods. One such method is making multiple layer membrane of Nafion and polypyrrole. Such membranes are called hybrid membranes. These membranes reduce the crossover of vanadium ions and improve the efficiency. In addition to this method, Nafion is modified with silica SiO_2 or titania TiO_2, and resulting Nafion/SiO_2 composite membranes reduce the permeability of vanadium ions and hence increase the performance of VRFBs. The only problem of these Nafion-based membranes is that they are costly. Hence, cost-effective polymer membrane with all desired properties is needed. Many hydrocarbon-based polymers such as sulfonated polyethyl ether ketone (SPEEK) are being examined.

Limitations of all vanadium redox flow batteries are as follows:

1. Crossover of vanadium ions takes between anolyte and catholyte through ion exchange membranes. In addition to the vanadium ions, water also gets transported along with selective balancing ions (H^+ as H_3O^+) across the membrane leading to water imbalance. The net water transfer causes the negative and positive electrolytes to go out of balance resulting in the loss of capacity.
2. During charging and discharging, concentration of the sulfuric acid electrolyte varies. When sulfuric acid concentration reaches higher than 5 M, VO^{2+} ions tend to form ion pair resulting in a larger complex.
3. In strong acid solutions, V ($^{+5}$) ions in VO_2^+ tend to exist as hydrated ion $[VO_2(H_2O)_3]^+$ which is converted to VO $(OH)_3$ with the increase in temperature. At higher acid concentrations, VO $(OH)_3$ is converted to V_2O_5 and gets precipitated in the electrolyte tubes, reservoirs, etc.
4. The precipitation of V_2O_5 on ion exchange membrane leads to degradation in the performance of the stack demanding periodical maintenance.
5. The optimum operating temperature for all vanadium redox flow battery system is limited to 10 to 40 °C with 2 M of vanadium concentration in both the anolyte and catholyte.
6. Due to high cost of the ion exchange membranes, the capital cost of all vanadium redox flow battery is about 2500 USD/kWh with an additional cost of periodical maintenance of 500 USD/kWh.

Current status of all VRFBs

Development of all vanadium redox flow batteries began in 1984 at the University of New South Wales, Australia and many patents describing the use of vanadium-based RFBs were filed in the USA and elsewhere. In 1985, Kazacos et al. filed patents in Australia and the USA with Unisearch Limited, UNSW. Since then, a number of developments took place in UNSW with its collaborators and other countries like Austria, Canada, Japan, China, and Thailand [23]. Subsequently, many VRFBs have been installed and commercialized through licensing or patenting by many manufacturers. Development of these VRFBs is briefly presented in Table 4. Among the two types of VRBs, only type I is studied in detail and some of the pilot-scale VRFB power plants that have been installed are listed in Table 4 [36].

At present, there are several manufacturers of VRFBs in addition to those listed in the Table 4 [38]. Renewable Energy Dynamics Technology Ltd. (REDT) has developed ENIFY, a VRFB system with varying ranges of power/energy stored from 5 kW/20 kWh to 20 kW/100 kWh. Golden Energy Fuel Cell Co., Ltd. (GEFC), China, established in 2003, is marketing raw materials for VRFBs including electrodes, membranes, electrolyte, and cell stacks, as well as complete systems of 2.5 kW to 3.75 kWh and 4 MW to 32 MWh. V-Fuel, Australia established in January 2005 has an exclusive worldwide license for type 2 vanadium redox flow batteries and produces VRFBs with a range of power outputs between 5 and 50 kW. Prudent Energy, China, established in 2007, is also engaged in design and manufacture of VRFB systems. Prudent Energy acquired all the assets, patents, trademarks, and employees of VRFB power systems, Canada. Prudent Energy Corporation, a Delaware Corporation with its headquarters located in Bethesda, MD, is a wholly owned subsidiary of JD Holding, Inc., which in turn is owned by prominent investors from the USA, Europe, and Asia. VRB®, VRB-ESS®, and VRB ENERGY STORAGE SYSTEM® are registered trademarks of JD Holding, Inc. JD Holding, Inc. is the owner of US Patent Nos. 6,143,443, 6,468,688, 6,562,514, 7,078,123, 7,181,183, 7,184,903, 7,227,275, 7,265,456, 7,353,083, 7,389,189, 7,517,608, and related foreign patents. Additional patent rights are pending [45]. Cellenium Company Ltd., founded in 2000, is the only company licensed to market in Thailand and has a number of inventions associated with VRFBs. In 2010, Gildemeister, Germany entered into the market of energy storage with the "CellCube"—a commercial vanadium redox flow battery solution with powers and capacities ranging from 10 kW/40 kWh to 1 MW/4 MWh. The CellCube systems were originally developed by Celltrom GmbH, and it was acquired by the Gildemaster for marketing and commercialization of CellCube in the USA and European markets [46]. Volterion GmbH in Germany, founded in 2015, is a new startup company, which produces

Table 4 Pilot-scale power systems of type I VRFB installed in various places

Sample no.	Year	Size of the system power/energy	Developers/place of installation	Applications	Details on patents/IPR/license for commercialization [18]
1	1996	200 kW/800 kWh	Mitsubishi Chemicals/Kashima-Kita Electric Power, Japan	Load leveling	In 1993, the primary patent holder, Unisearch Limited (Australia), issued license to Mitsubishi International Corporation and Kashima-Kita Electric Power Corporation
2	1996	450 kW/900 kWh	Sumitomo Electric Industries (SEI)/Tasumi Sub-station, Kansai Electric Power, Japan	Peak shaving	In 1998, Pinnacle VRB (Australia) acquired the VRB technology from Unisearch Limited (Australia) and issued license to SEI, Japan. Pinnacle also issued license to VRB Power Systems (Vanteck VRB technology corporation), Canada
3	2000	200 kW/1.6 MWh	SEI/Kansai Electric Power, Japan	Peak shaving	SEI obtained license from Pinnacle
4	2001	170 kW/1 MW	SEI/Hakkaido Electric Power Wind Farm, Japan	Wind turbine power output stabilization	SEI obtained license from Pinnacle
5	2001	1.5 MW/1.5 MWh	SEI/Tattori Sanyo Electric, Japan	Peak shaving and UPS	SEI obtained license from Pinnacle
6	2001	250 kW/500 kWh	VRB Power/Stellan Bosch University, South Africa	Peak shaving and UPS	VRB power systems obtained license from Pinnacle in 1998
7	2001	500 kW/5 MWh	SEI/GwanseiGakuin University, Japan	Peak shaving	SEI obtained license from Pinnacle
8	2001	45 kW/90 kWh	SEI/CESI, Milan, Italy	R&D about distributed power generation	SEI obtained license from Pinnacle
9	2003	500 kW/2 MWh	SEI/High-Tech factory, Japan	UPS/peak shaving	SEI obtained license from Pinnacle
10	2003	250 kW/1 MWh	Pinnacle VRB/Huxley Hill Wind Farm, King Island	Wind energy storage	Pinnacle VRB acquired the technology from Unisearch limited in 1998
11	2004	250 kW/2 MWh	VRB Power/Castle Valley, Moab, US-UT	Voltage support and rural applications	VRB power systems obtained license from Pinnacle
12	2005	4 MW/6 MWh	SEI, Tomamae, Hokkaido, Japan	Wind energy storage and stabilization	SEI obtained license from Pinnacle
13	2009		Prudent Energy VRB Systems, USA and China		In 2009, Prudent Energy VRB systems acquired the assets of VRB power systems and the acquisition includes the purchase of all patents and trademarks.
14	2010	18 kW/100 kWh	The Netherlands, Cellstrom GmbH/Vierakker		Cellstrom GmbH were assigned patents for the invention of VRB components such as Frame of the cell (patent no. 8815428), DC/DC converters used in VRB (9093845), VRB systems (20140072897 and 8568912)

and sells compact size VRFB systems with power and energy outputs between 2–30 kW and 6–50 kWh, respectively [47]. Golden Energy Century Ltd. (GEC), China, founded in 2011, markets electrolyte and membranes for VRFBs, as well as cell stacks and entire VRFB systems with power/energy capacity ranging from 2.5 kW/40 kWh to 5 kW/40 kWh. Ashlawn Energy in the USA, supported by the US Department of Energy SmartGrid, is working on networking of National Laboratories [38].

Other RFB systems

The thermodynamic reversible potential for various redox couples that are of technical importance to make RFB is shown below. As we can see, there are many possible combinations of different anode and cathode redox couples, for example, iron/chromium redox flow battery, vanadium/bromine redox flow battery, polysulfide/bromine redox flow battery, etc. However, most of these systems are being developed and tested at laboratory scale level. Only few systems have reached the level of pilot-scale development. Among them, the Zn/Br_2 (ZBB) and soluble lead redox flow battery (SLRFB) systems are attractive.

Iron–chromium redox flow batteries

The iron–chromium redox flow batteries (ICRFBs), first developed by NASA, is considered to be the first redox flow batteries since as prior to its development there was no RFB system developed albeit the concept of the storing

energy in electrolyte was known [37]. L.H. Thaller of NASA had considered various redox couples for the development of RFBs and selected Fe/Cr system due to its abundance and cost [48].

The ICRFBs are developed by employing soluble redox couples of Fe^{2+}/Fe^{3+} as cathode active material and Cr^{2+}/Cr^{3+} as anode active material in electrolyte. Hydrochloric acid is used as supporting electrolyte for the anolyte and catholyte which are prepared by dissolving the respective chloride salts of iron and chromium. The anolyte and catholytes are separated by an ion exchange membrane. During charging of the ICRFBs, ferric ions (Fe^{3+}) are reduced to ferrous ions (Fe^{2+}) at cathode and chromous ions (Cr^{2+}) are oxidized to chromic ions (Cr^{3+}) at cathode. During the discharge of ICRFBs, the reactions at anode and cathode are reversed. The charge and discharge reactions of the ICRFBs can be written as:

At cathode:

$$Fe^{3+} + e^- \rightleftharpoons Fe^{2+} \qquad E^o = 0.77 \text{ V vs.SHE}$$

At anode

$$Cr^{2+} \rightleftharpoons Cr^{3+} + e^- \qquad E^o = -0.41 \text{ V vs.SHE}$$

Cell reaction

$$Fe^{3+} + Cr^{2+} \rightleftharpoons Fe^{2+} + Cr^{3+} \qquad E_{cell} = 1.18 \text{ V}$$

The cell reaction offers a standard voltage of 1.18 V. ICRFB operates with either a cation or anion exchange membrane/separator and typically employs carbon fiber, carbon felt, or graphite as electrode material. The supporting electrolyte is hydrochloric acid. ICRFBs exhibit high charge and discharge efficiency of up to 95 %.

Current status of ICRFBs

Recently, Enervault Corporation, USA has developed, deployed, and tested a 250-kW, 1-MW per four ICRFB system [14, 49, 50]. Enervault has patented their Cascade redox flow battery system [49], and it is reported that their ICRFB has about 79 % of energy efficiency when operated at 40 mA/cm^2. The energy efficiency is found to decrease with the increase of operating current density. It is also reported that the battery system was integrated with solar power for peak power management. It is reported that it is the only MW-h scale ICRFB system in the world. It is also observed that the efficiency depends on the nature of flow field [14]. Zeng et al. have reported that the ICRFB with interdigitated flow field could deliver an energy efficiency of 80.7 % at 320 mA/cm^2 which is 8.2 % higher than the ICRFB with serpentine flow field [51].

Zn/Br_2 redox flow batteries

The ZBRFBs are developed by employing zinc metal as anode active material and bromide ions present in the zinc bromide electrolyte as active materials at cathode. During charging of the ZBRFBs, zinc metal gets deposited at the anode from $ZnBr_2$ electrolyte and bromine is formed at the cathode. Bromine is dissolved in the electrolyte. To avoid the direct reaction between Zn deposited at anode and bromine present in the electrolyte, a microporous separator is employed. Hence, two electrolytes and two pumps are used to operate the ZBRFBs. During discharge of the cell, zinc is oxidized at anode and bromine is reduced to bromide ions at the cathode. The actual chemical species present in the catholyte polybromide ions Br_n^- where $n = 3$, 5, or 7.

The charge and discharge reactions of ZBRFB are written as follows:

At anode:

$$Zn^{2+} + 2e^- \rightleftarrows Zn \qquad E^o = -0.76 \text{ V vs.SHE}$$

At cathode:

$$2Br^- \rightleftarrows Br_2 + 2e^- \qquad E^o = 1.09 \text{ V vs.SHE}$$

The overall cell reaction is:

$$Zn^{2+} + 2Br^- \rightleftarrows ZnBr_2 \qquad E^o = 1.85 \text{ V}$$

The ZBRFB employs aqueous solution of zinc bromide as electrolyte with agents added to reduce the activity of toxic bromine gas. To avoid the reduction of Br_2 at Zn electrode during charge, a porous separator is used between the anode and cathode. The liquid electrolyte is circulated with quarternary ammonium salts as complexing agents, for example, *N*-methyl-*N*-ethyl morpholinium bromide, *N*-methylpyrrolidinium bromide, etc. are used as complexing agents to reduce the toxic bromine vapor activity. Although the concept of zinc/bromine battery is known for than 100 years, their development was hindered due to the problems associated with the zinc electrode, namely, dendrite formation and high solubility of bromine in the electrolyte $ZnBr_2$. ZBRFB attracted much attention due to the high theoretical cell voltage and high energy density and the electrode reactions are highly reversible. This system is actually a hybrid system as the Zn electrode involves deposition of active material at the electrode during charging. During discharge, the Zn metal dissolves into the electrolyte and transported outside of the battery.

Current status of ZBRFBs

The major problems associated with the ZBRFB are dendrite formation, hydrogen evolution reaction, and safety. Despite

these problems, ZBRFB in the range between 50 and 500 kWh have been developed and demonstrated. Recently, RedFlow limited, Australia, have patented their ZBRFB technology and is a leading developer and manufacturer of zinc–bromine flow batteries. Currently, Redflow has deployed 80 units of ZBRFB at various locations in Australia, the USA, and elsewhere [52]. Recently, a single flow ZBB with improved energy density is reported. In these ZBRFBs, the liquid storage reservoir and cathode side of the pump are removed and a semisolid electrode is used as cathodes. Such a ZBRFB has shown a performance of 92 % with coulombic efficiency and 82 % of energy efficiency over 70 charge and discharge cycles [53].

Soluble lead redox flow batteries

In a conventional lead-acid battery based on sulfuric acid, solid $PbSO_4$ is reduced to solid Pb at the negative plate while solid $PbSO_4$ is oxidized to solid PbO_2 at the positive plate during charging and the reverse reaction takes place with the generation of solid $PbSO_4$ during discharge. By contrast, lead-acid batteries with lead salts dissolved in an electrolyte with two inert electrodes have been first reported by Fritz Beck. Fritz reported that lead and lead dioxide can be deposited from lead perchlorate salt dissolved in perchloric acid and called them "lead perchlorate cell" [41]. Recently, Pletcher et al. have reported a lead-acid battery called soluble lead redox flow battery [54–64]. Soluble lead redox flow battery is based on lead (II) methanesulfonate dissolved in methanesulfonic acid. The operating principle of the SLRFB is shown in Fig. 5. Pb^{2+} ions in solution are oxidized to lead dioxide at the positive plates and concomitantly reduced to metallic lead at negative plates, respectively, while charging. During its discharge, both deposited active materials at electrodes are dissolved back in to the solution as lead (II)-soluble species. These charge and discharge cell reactions can be written as follows.

At negative (anode) electrode:

$$Pb(CH_3SO_3)_2 + 2e^- \underset{\text{Discharge}}{\overset{\text{Charge}}{\rightleftharpoons}} Pb + 2CH_3SO_3^- \qquad E^o = -0.13 \text{ V vs.RHE}$$

At positive (cathode) electrode:

$$Pb(CH_3SO_3)_2 + 2H_2O \underset{\text{Discharge}}{\overset{\text{Charge}}{\rightleftharpoons}} PbO_2 + 2CH_3SO_3^- + 2H^+ + 2e^-$$

$$E^o = 1.49 \text{ V vs.RHE}$$

Overall cell reaction is:

$$2Pb(CH_3SO_3)_2 + 2H_2O \underset{\text{Discharge}}{\overset{\text{Charge}}{\rightleftharpoons}} Pb + PbO_2 + 4CH_3SO_3H$$

$$E^o = 1.62 \text{ V}$$

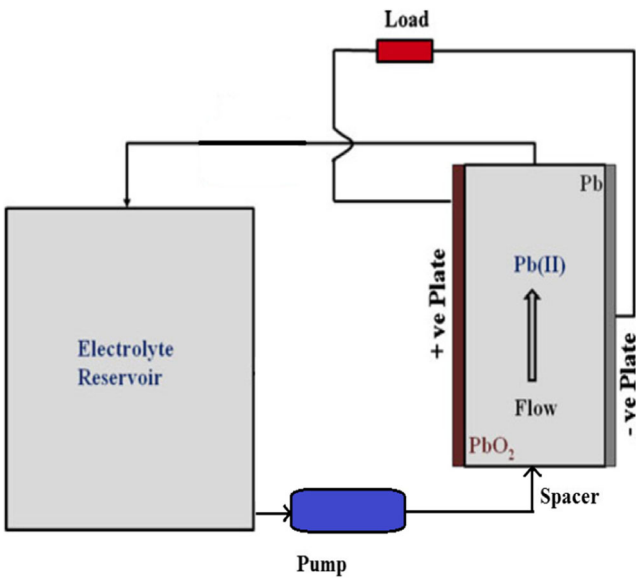

Fig. 5 A schematic representation of SLRFB

Electrolyte for SLRFB

The electrolyte used for SLRFB is prepared by dissolving 1.5 M lead methanesulfonate salt in 0.9 M methanesulfonic acid. No catalyst is required for charge and discharge reactions of SLRFB. However, the electrolyte is added with 0.1 wt% of sodium salt of lignosulfonic acid and 1 wt% of NaF. Additives are added to reduce dendrite growth and reduce oxygen evolution reaction during charging.

Electrode substrate

Graphite plates of required size are used as electrode substrate for both the anode and cathode for developing SLRFB. The positive surface of the monopolar and bipolar plates was designed with criss-cross structure. The negative surface of the monopolar and bipolar plates is 30 ppi glassy carbon foam embedded into the graphite plates.

Benefits of SLRFB

Electrode reactions are fast and offer high operating current density. The reactions are diffusion controlled. The energy efficiency is high with a long cycle life. Since a single electrolyte solution is used for both the anode and cathode, there is no need of an expensive ion-conducting membrane and two electrolyte reservoirs as in the case of VRFBs. SLRFBs use one electrolyte reservoir without an

ion exchange membrane and one pump for circulating the electrolyte during its charge and discharge.

Limitations of SLRFB

SLRFBs with the above substrate, electrodes, and electrolyte offer a good performance when it is operated at low current densities of 20–25 mA/cm^2. Although higher current densities are achieved with the above materials, they have low energy conversion efficiency and low cycle life. This is due to problems associated with the electrode reactions. The cathode potential of SLRFB 1.49 V vs. SHE at equilibrium is found to increase to about 1.8 V vs. SHE reaching the oxygen evolution reaction region on carbon electrodes. As a result, during charging of the SLRFB, the oxygen evolution reaction consumes part of the charge reducing the coulombic efficiency of PbO_2 deposition. At the same time, there is no decrease in the coulombic efficiency in the deposition of Pb metal. During the discharge reaction, almost all the PbO_2 could dissolve into the solution but at an anode a part of Pb metal remains. This imbalance in the charge and discharge reactions leads to the formation Pb dendrites at anode. If the SLRFB is operated at high current densities, oxygen evolution also occurs at higher rate leading to peeling and shedding of deposited PbO_2 active material causing accumulation of sludge at the bottom of each cell in the stack. As a result of these problems, the life cycle of the SLRFB is low at higher current densities. In addition to the sludge formation, the acid concentration increases about four times leading to poor solubility of Pb^{2+} ions.

Current status of SLRFB

The progress of SLRFB with its performance characteristics since it was reported by Pletcher et al. in 2004 is briefly summarized in Table 5 [54–64]. In essence, the solubility and conductivity of Pb^{2+} ions in methanesulfonic acid (MSA), single electrode performance characteristics by voltammetry using rotating disc electrodes, effect of additives, influence of flow cell operating conditions such as temperature, structural, and morphological studies on the deposits of Pb and PbO_2, and scaling-up of electrode area from 2 to 1200 cm^2 are highlighted in Table 5. It has been found from rotating disc electrode studies that both the lead and lead dioxide deposition are mass transport-controlled reactions. The operating current density range of the flow cell is between 10 and 50 mA cm^{-2}. The coulombic efficiency of the flow cell is found to decrease with an increase in discharge current density. Typically, the efficiency at 20 mA cm^{-2} is found to decrease to 50 % at 100 mA cm^{-2} of load current. No significant hydrogen evolution is observed at negative electrodes, but oxygen evolution reaction is observed as a competing reaction at cathode during charge of the flow cell. Important consequences of the oxygen evolution reaction are the increase in Pb^{2+} ion concentration in MSA leading to a decrease in solubility of Pb^{2+} ions that leads to formation of dendrites at negative electrode and accumulation of PbO_2 deposits at cathode. These effects are shown in Fig. 6. This shows the formation of sludge in the bottom of the electrolyte flow frames. Following issues were identified from these reports and are needed to be addressed for its further development.

1. The faradaic efficiency is found to decrease with an increase in the charging current density. This is due to oxygen evolution. At higher operating current densities, the cathode potential increases and hence there is an increase in the oxygen evolution reaction.
2. The faradaic efficiency is also found to decrease with long period of charge and discharge cycling.
3. There is gradual accumulation of metallic lead and lead dioxide resulting in the formation of dendrites. This short circuits the electrodes and hence limits the cycle life.
4. It is essential to decrease the rate of oxygen evolution reaction during charging of the flow cell by adding suitable additives to the electrolyte to prevent dendrite formation and PbO_2 accumulation.
5. Accumulation of PbO_2 at the inlet of the manifold needs to be prevented by suitable manifold designs.

Efforts are being expended to understand the PbO_2 deposition in MSA. Recently, Oury et al. have reported that an increase in proton concentration in MSA has adverse effect in passivating PbO_2 layer at the end of reduction [65]. In addition, there is formation of non-stoichiometric PbO_x with a poor solubility and high electrical resistance. The cathode also shows an activation polarization for oxidation of Pb^{2+} ion to PbO_2 in MSA. Despite these drawbacks, SLRFB show good cyclability for short periods of charge and discharge. Low cost, availability of raw materials, and easy design in manufacturing make SLRFB attractive for energy storage applications.

We at the Indian Institute of Science, Bangalore have developed and test performed a soluble lead redox flow battery with corrugated graphite sheet and reticulated vitreous carbon as positive and negative current collectors [66]. In the cell, electrolyte comprising 1 · 5 M lead (II) methanesulfonate and 0 · 9 M methanesulfonic acid with sodium salt of lignosulfonic acid as additive is circulated through the reaction chamber at a flow rate of 50 mL min^{-1}. During the charge cycle, pure lead (Pb) and lead dioxide (PbO_2) from the soluble lead (II) species are electrodeposited onto the surface of the negative and positive current collectors, respectively. Both the electrodeposited materials are characterized by XRD, XPS, and SEM. Phase purity of synthesized lead (II) methanesulfonate is unequivocally established by single crystal X-ray diffraction followed by profile refinements using

Table 5 Update of the progress in SLRFB since 2004

Year	Brief description of the work	Electrode	Electrolyte	Performance characteristics
2004	Preliminary studies on the Pb^{2+}/Pb and Pb^{2+}/PbO_2 couples in MSA by rotating disc electrode, cyclic voltammetry, and V-t performance	Vitreous carbon disc electrode	4 mM of Pb^{2+} ions in 2 M MSA for RDS and CV studies; 0.9 M Pb^{2+} ions in 1.5 M MSA for V-t studies	Solubility and conductivity tests carried out in order to develop SLRFB
2004	The design and performance characteristics of 2 cm^2 active area SLRFB is reported	Carbon power with HDPE binder	0.9 M Pb^{2+} ions in 1.5 M MSA for V-t studies	The single cell with 1.6 V is cycled over the range of 10–60 mA cm^{-2} for 1-h and 5-min durations. The single cell exhibited an 85 % coulombic efficiency and 65 % energy efficiency
2005	Effect of concentration, electrode support, flow rate, temperature, and SoC on the performance of SLRFB is reported	Carbon powder with HDPE binder on (i) Ni, (ii) RVC, and (iii) scrapped RVC support	Pb^{2+} ion in the range of 10 mM to 1.5 M dissolved in MSA at different contraptions in the range of 3.8 to 0.9 M	Accumulation of lead metal after cycling is reported. Also, the efficiency is found to decrease with the increase in operating current density. It is reported that the charge efficiency of 85 % at 20 mA cm^{-2} is reduced to 62 % at 100 mA cm^{-2}
2005	The influence of sodium lignosulfonate as additive at various concentrations is reported	Same as part III	0.9 M Pb^{2+} ions in 1.5 M MSA	0.1 % of sodium lignosulfonate is found to have an effective leveling agent. Efforts with inorganic additives were unsuccessful
2008	Detailed study on the negative electrode	Active area is increased to 8 cm^2 with carbon composite electrodes	0.9 M Pb^{2+} ions in 1.5 M MSA; effects of various additives are reported	Hexadecyltrimethylammonium cations are found to give good quality deposits of Pb
2008	Detailed study on the positive electrode	Active area is 8 cm^2 with carbon composite electrode	0.1–1.5 M lead (II) and MSA in the range 0–2.4 M + 5 mM hexadecyltrimethylammonium cation	Compact and well-adherent layers are reported with current densities >100 mA cm^{-2} in electrolytes containing
2009	Studies on PbO_2 deposits by SEM and XRD	Carbon electrode area of 1 cm^2	0.5 M Pb^{2+} ion in 0.5 M MSA at pH = 0.45	Effect of charge and discharge cycling on the PbO_2 deposits shows that it is possible to deposit either α-PbO_2 or β-PbO_2 or mixture of the two
2010	Development of SLRFB with 100 cm^2 active area	Positive electrode is carbon composite and negative electrode is Ni and carbon composites	0.5 M Pb^{2+} ion in 0.5 M MSA + 5 mM hexadecyltrimethylammonium cation	The cell is charged and discharged for various time durations. The efficiency is found to decrease with increasing the charge and discharge time. The decrease in performance is attributed to oxygen evolution increasing the concentration, dendrite formation, and poor adhesion of PbO_2
2010	Conditioning the electrolyte with H_2O_2	Positive electrode is carbon composite and negative electrode is Ni and carbon composites	0.5 M Pb^{2+} ion in 0.5 M MSA + 5 mM hexadecyltrimethylammonium cation	The long period cycling of the cell results in accumulation of Pb and PbO_2 leads the shorting between the two electrodes. Hence, a simple chemical method of dissolving these deposits by adding H_2O_2 periodically is reported
2012	Development of pilot-scale SLRFB	–	Pb^{2+} ions dissolved in high concentrations of MSA	There are five SLRFBs with each 1000 cm^2 active area reported. Each cell had an OCP of 1.8 V and can give an energy efficiency of 70 % with a life cycle of 100 cycles. The power density at 1.2 V is reported to be maximum at 160 mW cm^{-2}

high-resolution powder data. During the discharge cycle, electrodeposited Pb and PbO_2 are dissolved back into the electrolyte. Since lead ions are produced during oxidation and reduction at the negative and positive plates, respectively, there is no risk of crossover during discharge cycle, which prevents the chances of lowering the overall efficiency of

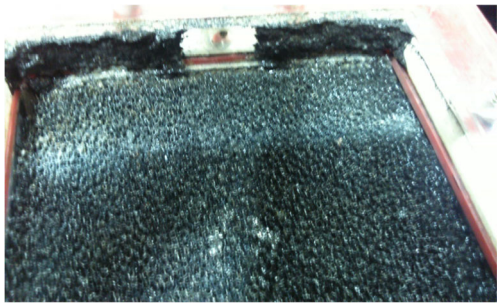

Fig. 6 Formation of sludge in the bottom of the electrolyte flow frames

the cell. As the cell employs a common electrolyte, the need of employing a membrane is averted. It has been possible to achieve a capacity value of 114 mAh g^{-1} at a load current density of 20 mA cm^{-2} with the cell at a faradaic efficiency of 95 %. The cell is tested for 200 cycles with little loss in its capacity and efficiency.

Verde et al. have developed SLRFBs with more than 2000 cycle life at 20 mA cm^{-2} current density [67]. This research group from the University of California, San Diego (USA) in collaboration with General Atomics is currently engaged in the development of 20-kW SLRFB employing low-cost materials and a simpler design with a target of $100/kW for grid-scale applications.

We have demonstrated corrugated graphite and glassy carbon foam suitable positive and negative flow fields for soluble lead flow battery [66]. Corrugated graphite surface provides higher surface area to electrode and increases the adhesion of fine lead dioxide particles. High surface area of glassy carbon foam helps in efficient electrodeposition of metallic lead. A 2-V single cell with 3.5 cm × 3.5 cm electrodes is fabricated and performance was tested. Addition of lignosulfonic acid sodium salt to the electrolyte solution minimizes the dendrite growth of lead depositions. A cycle life in excess of 200 cycles obtained from the 2-V single cell studies is shown in Fig. 7.

Subsequently, the cell that has been scaled up to a 12-V/50-Wh soluble lead redox flow battery stack with bipolar plates with corrugated graphite and glassy carbon foam as positive and negative flow fields, respectively, is shown in Fig. 8. The faradaic efficiency of SLRFB is 85 % when it is charged for 15 min at 1A, and it is 65 % when the charged for 3 h. Similarly, the faradaic efficiency decreased to 60 % when the SLRFB is charged at 5A for 15 min duration. Hence, long period of constant current charging and charging at higher current charging leads to a decrease in overall efficiency of the flow cell. The decrease in efficiency is attributed to the accumulation of active materials in the stack specifically PbO_2. The accumulation of PbO_2 leads to electrical shorting between the cells. Further optimization of the performance work is in progress.

Constant current discharge data for this SLRFB is shown in Fig. 9, and the current–potential performance behavior is shown in Fig. 10. The work on integrating the 50-W SLRFB with a solar panel to charge the SLRFB with solar energy is also in progress; this will be scaled to 500-W SLRFB and performance will be tested subsequently.

Redox flow batteries with nonaqueous electrolytes

Nonaqueous electrolytes have large electrochemical potential working range than the aqueous electrolytes. Hence, RFBs with nonaqueous electrolytes have the ability to offer high cell voltage and thus can offer higher energy density. In addition, the salts which are not soluble in water could dissolve in nonaqueous solvents. The working principle of the RFBs with nonaqueous electrolytes is exactly similar to that of aqueous electrolyte RFBs. The most commonly employed solvents are acetonitrile, dimethylsulfoxide, propylenecarbonate, and dioxalane-based electrolytes. The metal salts have poor solubility in these solvents and hence in order to increase their ionic conductivity supporting electrolytes such as triethylammonium tetraflouroborate ($TEABF_4$), Triethylammonium hexaflourophosphate ($TEAPF_6$) is added to improve their ionic conductivity. RFBs with nonaqueous electrolyte and polymer-based materials are classified into four categories [40, 68]:

1. RFBs with metal complexes dissolved metal complexes such ML_6 where *M* is transition metal and *L* is a ligand. The most commonly employed metal complexes are Ru, V, Mn, and Cr with acetylacetonoate, bipyridyl ligands
2. All organic redox flow batteries: In this type of RFBs, organic compounds or stable organic radicals are used as active materials by dissolving in organic solvents. For example, 2,2,6,6-tetramethyl-1-piperidinyloxy (TEMPO) and *N*-methylphtalimide dissolved in acetonitrile supported by $NaClO_4$ are used as catholyte and anolytes.
3. Lithium-based redox flow batteries
4. Aqueous, polymer-based redox flow batteries: Recently, Schubert et al. reported a new class of organic redox flow batteries that employ organic water-soluble polymers as active materials and inexpensive dialysis membranes as separators for anolyte and catholyte [40]. The active materials comprising polymers consist of two components: a redox-active moiety and a unit to enhance solubility in water. An example of such a RFB is one using TEMPO radical as cathode active moiety and 4,4′-bipyridine derivative (Viologen) as anode material. In this system, while charging the TEMPO radical is oxidized to oxammonium ($TEMPO^+$), viologen cation ($Viol^{2+}$) is reduced to monovalent radical cation ($Viol^+$). During the discharge, reverse reaction takes place. Such an aqueous and polymer-based RFB has an energy density of 10 Wh/L and current densities as high as 100 mA/cm^2.

RFBs with metal complexes

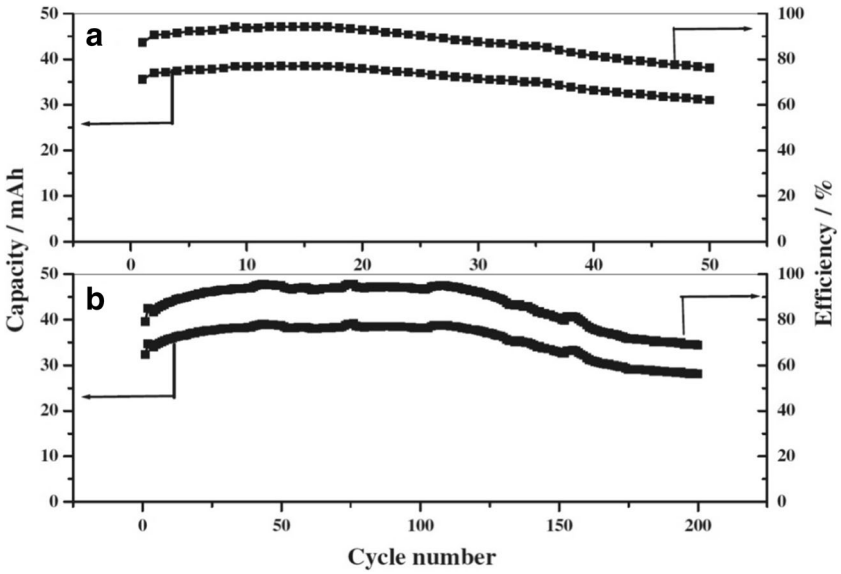

Fig. 7 Cycle life data (capacity and efficiency of cell vs. cycle number) for SLRFB **a** without additive and **b** with sodium lignosulfonate additive

The operating principle of a RFB with metal complexes dissolved in nonaqueous electrolyte is same as in the case of aqueous electrolyte RFB. The anolyte and catholyte can have either the same metal complex or different complexes. Usually, the same metal complexes are employed. During the charging and discharging, the metal ions of the complex undergo oxidation or reduction reaction and ligand remains unaffected. In such a case, the energy density of the RFB depends on the concentration of the metal complex. However, in rare cases, the ligands also participate in redox reactions. In such cases, the energy density is calculated by taking into account the charge transferred from ligands as well.

A typical example for the RFBs with metal complexes is Ru complexes of bipylidyl (bpy) and acetylacetenoate (acac) dissolved in acetonitrile with $TEABF_4$ electrolytes. The redox reactions of such RFBs are as follows:

At cathode:

$$\left[Ru(bpy)_3\right]^{2+} \rightleftarrows \left[Ru(bpy)_3\right]^{3+} + e^- \qquad E^o = 1.0\ \text{V vs.Ag}/\text{AgCl}$$

At anode

$$\left[Ru(bpy)_3\right]^{2+} + e^- \rightleftarrows \left[Ru(bpy)_3\right]^{+} \qquad E^o = -1.6\ \text{V vs.Ag}/\text{AgCl}$$

The overall cell reaction is,

$$2\left[Ru(bpy)_3\right]^{2+} \rightleftarrows \left[Ru(bpy)_3\right]^{3+} + \left[Ru(bpy)_3\right]^{+} \qquad E^o = 2.6\ \text{V}$$

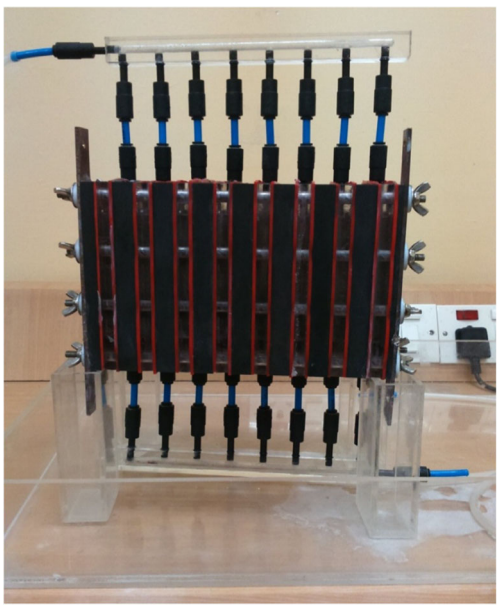

Fig. 8 A 12-V/50-W SLRFB stack with eight cells in series and each cell has an active area of 10 cm × 10 cm

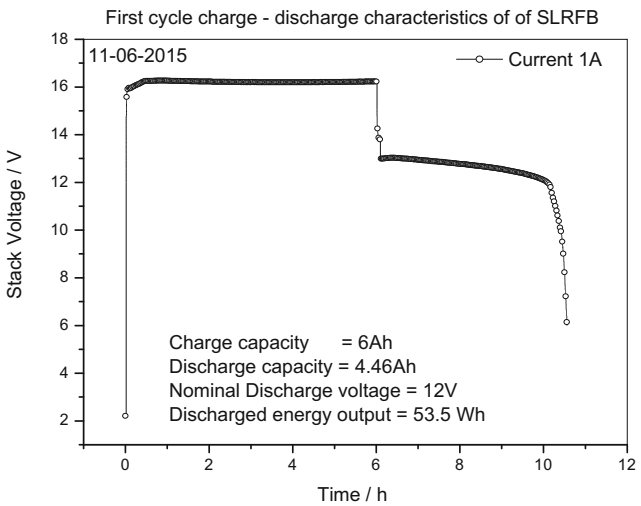

Fig. 9 Constant current charge and discharge data for 12 V/50 W SLRFB

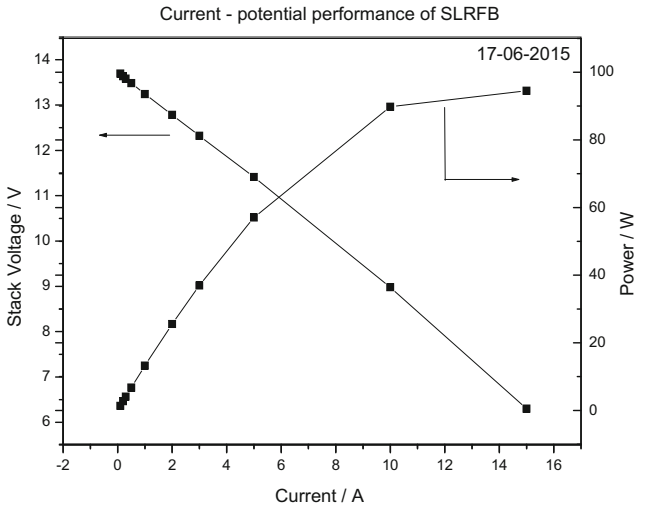

Fig. 10 Performance data for the 12-V/50-W SLRFB

In this kind of redox flow batteries, porous separators filled with ion exchange membranes are used. In the above case, a sintering glass filter with anion exchange membrane is used. Membranes for such RFBs are prepared by various methods such as solution casting method, pore-filled ion exchange resin method, and γ-radiation grafting method. A typical example of anion exchange membrane, poly(pthalazinone ether sulfone ketone), PPESK, is prepared by the following method. In the first step, PPESK-polymer was subjected to chloromethylation with a catalytic agent to obtain [PPESK] CH_2Cl polymer. This is then aminated with trimethylamine and the Cl^- ion exchanging resin is obtained.

1. [PPESK]-CH_2Cl ➔ [PPESK]$CH_2N(CH_3)_3Cl$

One of the problems of this kind of nonaqueous RFBs is low solubility of the metal complexes. Hence, they have poor energy density. RFBs with different metal complexes at anode and cathode are also reported in literature. An example of such system is shown in Fig. 11.

2. Lithium-based redox flow batteries

It is known that Li-ion batteries have high operating voltages and high theoretical energy density. There are two possible ways in which we can realize lithium RFBs and get the benefits of high energy density of lithium batteries. In one method, electrolytes with suspensions of conventional lithium anodes and cathode materials are used to realize Li RFBs. It is a semisolid type suspension containing ion-storing insertion materials. In this method, the challenge lies in the incorporation of electrically conductive additives, so that the percolation threshold of the electrolyte is exceeded. The addition of large amounts of electrically conductive carbon blacks, such as Ketjen Black, frequently results in the suspensions being viscous and difficult to pump. A bare lithium anode, however, like all lithium metal anodes, tends to undergo dendrite formation during metal deposition. A microporous polymer separator was used to prevent the crossover of negative and positive active materials. The catholyte used in the first lithium-flow battery was a suspension of $LiCoO_2$ (20 vol%; 10.2 M) with 1.5 % Ketjen Black. The anolyte used was a suspension of $Li_4Ti_5O_{12}$ (10 vol%; 2.3 M) with 2 % Ketjen Black. The battery was tested without electrolyte convection and achieved a current efficiency of 73 and 80 % for the first two cycles. Suspension batteries, because of their solid content, usually have a higher theoretical energy density than those based on solutions. The authors expect energy densities of about 130–250 Wh kg^{-1} in an optimized system. Due to the solid nature of the suspending flow able electrode material, the equivalent concentrations of positive electrode suspensions such as $LiCoO_2$ and $LiNi_{0.5}Mn_{1.5}O_4$ and negative electrode suspensions such as $Li_4Ti_5O_{12}$ and graphite are 51.2, 24.1, 22.6, and 21.4 mol/dm^3, respectively, which are significantly higher than those of RFBs (<5 mol/dm^3). This resulted in an increase in the energy density per electrolyte volume to approximately 10 times that of a VRFB.

The other forms of Li RFBs are a metallic lithium anode, an ion-permeable protective layer, and an organic catholyte in which the redox-active substance is dissolved. A semi-aqueous semi-organic Li-RFB was described by Lu and Goodenough. The battery contained an aqueous $[Fe(CN)_6]^{3-}/[Fe(CN)_6]^{4-}$ solution as catholyte and $LiPF_6$ in an equal mixture of ethyl carbonate and diethyl carbonate as anolyte. The half cells were separated by a $Li_{1+x+y}Al_xTi_{2-x}Si_yP_{3-y}O_{12}$ membrane material. This material has a structure similar to Nasicon/Lisicon and has high Li^+ ionic conductivity. The selection of $[Fe(CN)_6]^{3-}/[Fe(CN)_6]^{4-}$ as the positive redox species, the lithium-ferricyanide flow battery, gives an effective voltage between 3.33 and 3.68 V at 0.5 mA cm^{-2}. Four different flow rates were tested. The highest flow rate (0.41 mL min^{-1}) delivered a power density of 17 mW cm^{-2}. A coulombic efficiency of more than 97 % is also achieved over 1000 cycles. However, the limitation of this system is the low current density (<2.5 mA cm^{-2}) due to the deterioration of the solid electrolyte separator. Also, the low mobility of lithium ion in the solid electrolyte separator can increase the resistance significantly. Aiming for larger power output and extended life time, the lithium ion conductivity and the chemical resistance properties of the solid electrolyte separators need further improvements.

Significance and applications of RFBs

The significance of RFBs lies in the fact that these are one of the best-suited electrochemical energy storage systems

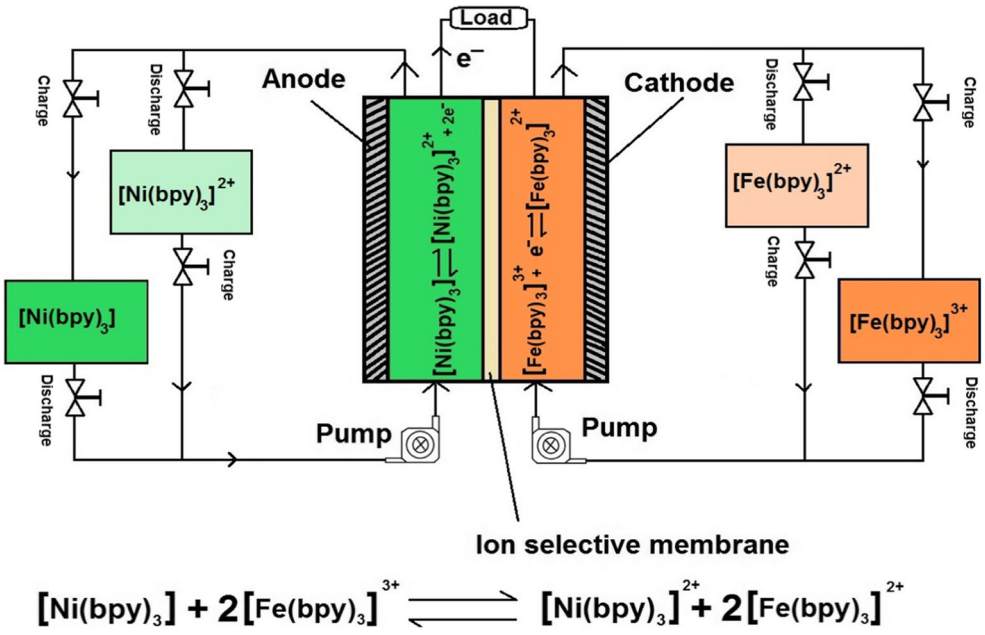

Fig. 11 Operating principle of a RFB with metal complexes dissolved in nonaqueous electrolyte

for developing the local grids. As mentioned earlier, RFBs have the advantage over other electrochemical systems. An attractive feature of the RFB systems is that the power and energy density are independent of each other in contrast to batteries and supercapacitors. This special feature helps in building RFB systems as large-scale energy storage systems suitable for developing local grid network. Techno-economic features of some prospective electrochemical energy storage systems and VRFBs are compared in Table 6.

Although supercapacitors have high cycle life, their energy density is less and hence they are not suitable for large-scale energy storage applications. Among the batteries, lead-acid and Li-ion batteries only are available in commercial market. Li-ion batteries are expensive and also have inherent safety problems for large-scale energy applications. Although both NaS and VRFB have desired characteristics, they are still expensive. The lead-acid batteries are cost-competitive, but they have low cycle life particularly in deep discharge cycles. A compelling option is therefore to develop a redox flow battery-based lead-acid battery system as it can meet the desired cycle life and is economical. A typical objective of SLRFB is to have 10,000 cycles with an estimated cost of US$100/kWh. There are many applications of RFBs as electrical energy storage system in the development of nano and micro grids. Few of these are peak shaving, time shifting (arbitrage), load leveling, voltage regulation and control, low voltage ride through, emergency backup, transmission and distribution services, telecommunication backup, EV charging, seasonal energy storage, black start, grid network fluctuation suppression, and many more.

Market prognosis

The demand for large-scale energy storage systems depends on widespread utilization of renewable energy sources in micro grids. The renewable electricity generation is expected to grow by 45 % between 2013 and 2020, reaching 7310 terrawatt hours (TWh) [7]. A range of possibilities exists for the deployment of large-scale energy storage systems over the next decade. The level of investment required in energy storage technologies depends on various scenarios from an estimated USD 380 billion to 750 billion in the USA, China, India, and Europe alone [6]. These investments' needs are just a fraction of the USD 18 trillion investments needed in power generation in 2DS in these four regions [6]. A recent report suggests that revenue from the distributed energy storage systems is expected to exceed $16.5 billion and revenue from grid-scale energy storage is expected to exceed $68 billion by 2024 [69, 70]. Another research report suggests that low-cost flow batteries are expected to create $190 million energy storage market by 2020 [71]. Market prospects for energy storage systems look truly promising for the next decade. Flow batteries may constitute a small part of the energy storage systems market, but they are a promising long-term storage solution due to their ability to meet the requirement of large energy capacity.

India has the third largest energy demand in the world after China and the USA. With the electricity demand in India expected to grow more than double in the next decade, the power sector faces two main challenges, namely, adequately powering projected economic growth and bringing electricity to the 300 million citizens who currently lack or have no access to electricity [72]. Moreover, India has announced a

Table 6 Cost and performance comparison for some prominent storage technologies

Electrochemical system	Typical power size MW	Discharge time	Life cycle	Estimated cost kWh USD	Cost of storage/kWh USD
Supercapacitors	0.25	<1 min	500,000	3000	–
Lead-acid batteries	0.5–20	3–5 h	1000/3 years	100	0.1
NaS batteries	0.25–1	6–8 h	2500/6 years	500	0.2
Vanadium RFBs	0.5–12	10 h	1000/10 years	500	0.5

target to achieve 15 % share of renewable energy by 2020. This demands substantial renewable energy technologies to be integrated with the national grid. It is reported that India is planning to deploy solar energy power plants to the tune of 100 GW by 2022 of which 2.2 GW will be for grid-connected wind and solar farm integration [73, 74].

Technical challenges

The most challenging problem associated with the development of RFB systems is relatively higher cost of production and periodical maintenance in comparison to other EES like pumped hydroelectric energy storage systems. Although VRFB systems have reached pilot-scale production and demonstrated their suitability for micro grid applications, they need periodical maintenance of membranes and electrode materials. The levelized cost of energy (LCOE) can be lowered by increasing the number of charge and discharge cycles of RFBs. Lowering the cost of VRFBs and increasing their life cycle span must be achieved with the choice of electrode and membrane materials. In the case of ICRFBs, the hydrogen gas evolution at iron electrode is a serious issue. The performance degradation of the membrane adds cost to the ICRFB maintenance. ZBB suffers due to the formation of dendrites. In the case of SLRFB, the oxygen evolution at cathode during charging leads to the imbalance in the chemical composition of the electrolyte. Formation of dendrites at the anode and unreacted PbO_2-forming sludge in electrolyte inlet region of the spacer are technical problems associated with SLRFB.

Conclusions

Global warming due to the continuous exploitation of fossil fuel-based power generation is forcing us to utilize renewable energy sources. The significance of developing local grid along suitable energy storage system to integrate the RES is discussed. Redox flow batteries are expected to play a seminal role as large-scale energy storage systems in the local grid network. We have reviewed the operating principles of different types of redox flow batteries with special interest to systems which have reached pilot-scale production. The merits and demerits of VRFB and its electrode reactions are discussed in detail. The status of ICRFB, ZBB, and SLRFB is also presented. Research reports suggest that RFBs will have market prospects of 190 million US dollars in the next decade.

References

1. Gielen D (2008) Energy technology perspectives scenarios & strategies to 2050, OECD. International Energy Agency, France
2. Chu S, Majumdar A (2012) Nature 488:294–303
3. SGIP White Paper on Local Grid Definitions (2016) http://www.sgip.org. Accessed 02 Feb 2016
4. Martínez FM, Miralles AS, Rivier M (2016) Renew Sust Energ Rev 62:1133–1153
5. Off-grid renewable energy systems: status and methodological issues (2015) International Renewable Energy Agency. http://www.irena.org. Accessed 2015
6. Technology Roadmap Energy Storage (2014) OECD/IEA France. Accessed 2014
7. Tracking Clean Energy Progress (2015) Energy technology perspective OECD IEA France. Accessed 2015
8. Grid Energy Storage (2013) Department of Energy. http://energy.gov/oe/downloads/grid-energy-storage. Accessed Dec 2013
9. Electrical Energy Storage (2011) White paper, International Electrotechnical Commission Switzerland. Accessed 2011
10. Skyllas M, Kazacos MH, Chakrabarti SA, Hajimolana FS, Saleem M (2011) J Electrochem Soc 158:R55–R79
11. Zakari B, Syri S (2015) Renew Sust Energ Rev 42:569–596
12. Electricity energy storage technology options (2010) A white paper primer on applications costs and benefits EPRI, USA. Accessed 2010
13. Rudolf Holze Springer handbook of electrochemical energy (2017), Series Springer Handbooks, C. Breitkopf, K. Swider-Lyons (Eds.), 1st ed., 591–610.
14. Craig H, Ron M, Taylor S, Bret A (2014) Demonstration of Enervault iron–chromium redox flow battery. California Energy Commission
15. J. Jorne (1983) American scientist, Sept–Oct.: 507
16. Bartolozzi M (1989) J Power Sources 27:219–234
17. Tokuda N, Kanno T, Hara T, Shigematsu T, Tsutsui Y, Ikeuchi A, Itou T, Kumamoto T (2000) SEI Technical Review 50:89–93
18. León CP, Ferrer AF, García JG, Szánto DA, Walsh FC (2006) J Power Sources 160:716–732
19. Wills RGA, Collins J, Campbell DS, Low CTJ, Pletcher D, Walsh FC (2010) J Appl Electrochem 40:955–965
20. Noack J, Tübke J (2010) ECS Trans 25:235–245
21. Zhang HM (2010) ECS Trans 28:1

22. Nguyen T, Savinell RF (2010) Interface Fall S4:54–56
23. Kear G, Shah AA, Walsh FC (2011) Int J Energy Res 36:1105–1120
24. Soloveichik GL (2011) Annu Rev Chem Biomol Eng 2:503–527
25. Yang Z, Zhang J, Meyer MC, Lu X, Choi D, Lemmon JP, Liu J (2011) Chem Rev 111:3577–3613
26. Weber AZ, Mench MM, Meyer JP, Ross PN, Gostick JT, Liu Q (2011) J Appl Electrochem 41:1137–1164
27. Shigematshu T (2011) SEI Technical Review 73:4–13
28. Li L, Kim S, Wang W, Vjayakumar M, Nie ZB, Zhang J, Xia G, Hu J, Graff G, Liu J, Yang Z (2011) Adv. Energy Mater 1:394–400
29. Leung P, Li X, León CP, Berlouis L, Low CTJ, Walsh FC (2012) RSC Adv 2:10125–10156
30. Shibata T, Kumamoto T, Nagaoka Y, Kawase K, Yano K (2013) SEI Technical Review 76:15–21
31. Toshikazu S, Takahiro K, Yoshiyuki N, Kazunori K, Keiji Y (2013) Energy Storage Science and Technology 2:233–236
32. Wang W, Luo Q, Li B, Wei X, Li L, Yang Z (2013) Adv Funct Mater 23:970–986
33. Chakrabrti MH, Hajimolana SA, Mjalli FS, Saleem M, Mustafa L (2013) Arab J Sci Eng 38:723–739
34. Parasuraman A, Lim TM, Menictas C, Kazacos MS (2013) Electrochim Acta 101:27–40
35. Chalamala BR, Soundappan T, Fisher GR, Anstey MR, Viswanathan VV, Perry ML (2014) Redox flow batteries: an engineering perspective. Proceeding of the IEEE. doi:10.1109/JPROC.2014.2320317
36. Alotto P, Guarieri M, Moro F (2014) Renew Sust Energ Rev 29: 325–335
37. Noack J, Roznyatovskaya N, Herr T, Fischer P (2015) Angew Chem Int Ed 54:9776–9809
38. Cunha A, Martins J, Rodrigues N, Brito FP (2015) Int J Energy Res 39:889–918
39. Soloveichik GL (2015) Chem Rev 115:11533–11558
40. Janoschika T, Martin N, Martin U, Friebe C, Morgenstern S, Hiller H, Hager MD, Schubert US (2015) Nature 527:78–81
41. Janoschika T, Hager MD, Schubert US (2012) Adv Mater 24:6397–6409
42. Winsberg J, Janoschika T, Morgenstern S, Hagemann T, Muench S, Hauffman G, Gohy J–F, Hager MD, Schubert US (2016) Adv Mater 28:2238–2243
43. Fritz Beck, (1977) US Patent No 4001037
44. Kim KJ, Park MS, Kim YJ, Kim JH, Dou SX, Skyllas-Kazacos M (2015) J Mater Chem A 3:16913–16933
45. http://www.pdenergy.com/intellectual-property.php. Accessed on October 28 2015
46. The German American Flow Battery Connection (2014). http://www.greentechmedia.com/articles/read/the-german-american-vanadium-flow-battery-connection. Accessed 24 Feb 214
47. https://datafox.com/volterion. Accessed on October 10 2016.
48. Thaller LH (1976) Electrically rechargable redox flow cell. US patent 3:996,064
49. Horne CR, Kinoshita K, Hickey DB, Sha JE, Bose D (2014) Cascade redox flow battery system, US patent 8,785,023B2.
50. Long Duration Grid Scale Iron Chromium Redox Flow Battery (2010) http://www.sandia.gov/ess/docs/pr_conferences/2014. Accessed 28 Oct 2010
51. Zeng YK, Zeng XL, Zhou L, Zeng XH, Yan TS (2016) J Power Sources 327:258–264
52. Red Flow Advanced Energy Storage (2015). http://redflow.com/wp-content/uploads/2012/08/RedFlow-Limited-August-Update.pdf. Accessed 28 Oct 2015
53. Lai Q, Zhang H, Li X, Zhang L, Cheng Y (2013) J Power Sources 235:1–4
54. Hazza A, Pletcher D, Wills R (2004) Phys Chem Chem Phys 6: 1773–1778
55. Pletcher D, Wills R (2004) Phys Chem Chem Phys 6:1779–1785
56. Pletcher D, Wills R (2005) J Power Sources 149:96–102
57. Hazza A, Pletcher D, Wills R (2005) J Power Sources 149:103–111
58. Pletcher D, Zhou H, Kear G, John CTL, Walsh FC, Wills RGA (2008) J Power Sources 180:621–629
59. Pletcher D, Zhou H, Kear G, Low CTJ, Walsh FC, Wills RGA (2008) J Power Sources 180:630–634
60. Li X, Pletcher D, Walsh FC (2009) Electrochim Acta 54:4688–4695
61. Collins J, Kear G, Li X, Low CTJ, Pletcher D, Tangirala R, Stratton D, Walsh FC, Zhang C (2010) J Power Sources 195:1731–1738
62. Collins J, Kear G, Li X, Low CTJ, Pletcher D, Tangirala R, Stratton D, Walsh FC, Zhang C (2010) J Power Sources 195:2975–2978
63. Wills RGA, Leon C, Walsh FC (2011) EESAT Conference. Oct. 16–19, San Diego Marriot Marquis Hotel, San Diego, USA
64. Ferrer AF, Garcia JG, Szánto DA, León CP, Walsh FC (2006) J Power Sources 160:716–732
65. Oury A, Kirchev A, Bultel Y, Chainet E (2012) Electrochim Acta 71:140–149
66. Banerjee A, Saha D, Row TNG, Shukla AK (2013) Bull Mater Sci 36:163–170
67. Verde MG, Carroll KJ, Wang Z, Sathrum A, Meng YS (2013) Energy and Environ Sci 6:1573–1581
68. Shin SH, Yun SH, Moon SH, (2013) RSC Advances, 3: 9095–9116
69. Revenue from Grid Scale Energy Storage (2015) Navigant Research. https://www.navigantresearch.com. A press release dated on 6 Jan 2015
70. Revenue from Distributed Energy Storage Systems (2015) Navigant Research. https://www.navigantresearch.com. A press release dated on 12 Jan 2015
71. Lower Cost Flow Batteries (2014) Luxresearch. http://www.luxresearchinc.com. Accessed on 9 Dec 2014
72. USAID (United States Agency for International Development) report on Assessment of the role of energy storage technologies for renewable energy deployment in India (2014). http://www.pace-d.com. Accessed March 2014
73. Battery storage for renewable: market status and technology outlook, International Renewable Energy Agency (IRENA) (2015). http://www.irena.org. Accessed on January 2015
74. Renewable and Electricity Storage (2015) International Renewable Energy Agency (IRENA). http://www.irena.org. Accessed June 2015